الجمـــهوريـــة الجـــزائريـــة الديـمقـراطيـــــــة الشـــعبيـــــة
PEOPLE'S DEMOCRATIC REPUBLIC OF ALGERIA

وزارة التعـلـيـم الـعـالـــي والـبـحـث الـعـلـمي
MINISTRY OF HIGHER EDUCATION AND SCIENTIFIC RESEARCH

جـامـعـة عمّـــار ثـلـيـــجـــي بالأغـــواط
UNIVERSITY AMAR TELIDJI LAGHOUAT

كـلـيـــــة الـعـلـــــوم
FACULTY OF SCIENCES

DEPARTMENT Science of Matter

Master memory

Domain: Sciences of matter
Field: Physics
Option : Material physics

By :

Miss:Gana Hadjer

THEME

$Mg_2Si_{1-X}Sn_X$, a case Study of pressure effects on a thermoelectric material

Supported publicly before the jury composed of:

Mr GUIBADJ Abdennceure	Prof	President
Mr SOULAH Kouidri	M.A.A	Examiner
Mr MAABED Said	M.A.A	Examiner
Mr LAGOUN Brahim	M.C.A	Advisor
Mr MARFOUA Brahim	Phd .Stud	Co-Advisor

University Year 2017- 2018

Dedication

No dedication can express the love, esteem, dedication and respect I have always had for you. Nothing in the world is worth the efforts provided day and night for my education and my well being. This work is the result of your sacrifices you made for my education and training. To you my father **Gana Mouhamed**

My mother **Rachedi Kaltoume** , who has worked for my success, by her love, her support, all the sacrifices made and her precious advice, for all her assistance and her presence in my life, receive through this work as modest as it is, expression of my feelings and my eternal gratitude.

To all my brothers and sisters: **Fatima, tourkiai, tadelja, masouda, aissa, boulafaa, badrdin**, and **houriai** My aunt **Aoiali** and to all my family **Gana**

My friends around the world who have been encouraging me khaoula, aicha, soumia, anfal, iman, afaf, iman, maroi, amina, souaad, marai, om amer, awatif, fatima, fadela M, baga L, …….

And especially to my professor Hamdi Rekai

To all students of the 2017/2018 class

To all my girlfriends of the two options: Physical matter sciences and chemistry.

…HADJER…

ACKNOWLEDGEMENTS

I thank above all **ALLAH** *the Almighty who offered me will, patience and Health, allowing me to carry out this work. And I thank my* **parent**.

First of all, I would like to express my deepest thanks to my mentor, **Mr. Lagoun Brahim**, *for his advice on the treatment of my memory topic, the rigor that guided his supervision and the long moments spent. to correct the memory, have been really appreciated.*

I warmly thank **Mr. Marfoua Brahim,** *who has done me the honor of being co-director of this memoir. I express my gratitude and gratitude for the clarity of his explanations.*

I express my gratitude to **Mr GUETBADJI Abdennceure**, *for having done me the honor of chairing the jury of this memoir. I want to express my gratitude to* **SOUALAH Kouidri** *and* **MAABED Said** *for accepting to be reviewers of this work.*

I extend my warm thanks to all the members of the Laboratory of Materials Physics at the University of Laghouat, especially its director **Mr. LEFKHEIR Ibn-Khaldoun**. *Their help allowed us to lead to good calculations.*

I thank all the teachers in the Department of Subject Sciences who have enriched my training.

Finally, I would like to express my thanks to my family and all my colleagues and friends

Summaries

CHAPTER III: Results and Discussions

Nomenclature

Symbols	Definitions
Q	The amount of heat
τ	Thomson coefficient
π	Peltier coefficient
COP	Coefficient of performance
ε_c	Coefficient of performance of Carnot
ZT	Dimensionless figure of merit
σ	Electrical conductivity
α	Seebeck coefficient
λ	Thermal conductivity
λ_l	Lattice thermal conductivity
λ_e	Electric thermal conductivity
ρ	Electrical resistivity
$S^2\sigma$	Power factor
T	Absolute temperature
N	Carrier concentration
$\tau_{n,\,p}$	The relaxation time
μ	Carrier mobility
e	Unit of charge carrier
I	Electrical current
T_C	Cold side temperature
T_H	Hot side temperature
η_H	Efficiency of power generation
η_C	Efficiency of cooling system
L	Lorentz number
V	Thermoelectric voltage
DFT	Density functional theory
GGA	Generalized gradient approximation
PAW	Projected augmented wave
XC	Exchange-correlation
Mg_2Si	Magnesium silicon
Mg_2Sn	Magnesium tin
LDA	Local Density Approximation

mBJ	Modified Becke-Johnson
LAPW	Linearized Augmented Plan Waves
f_k	The population group velocity
H	Hamiltonian
Ψ	wave function
E	Energy
R	Nucleus vector position
r	Electron vector position
T	kinetic energy
U	Potential energy
Z	Nucleus charge
n	Electronic density
DOS	Density of states
PBE	Perdew-Burke-Ernzerhof
B	Compression modulus
P	Pressure
BoltzTraP	Boltzmann Transport properties

List of Figures

CHAPTER 1

CHAPTER 2

CHAPTER 3

List of Table

CHAPTER 1

CHAPTER 2

CHAPTER 3

General introduction

General introduction

The physics of condensed matter and materials science are playing an increasingly important role in technological applications, and this role will only advance in many areas. Before using materials (solids) in industry, it is necessary to ensure the quality of their structural, electronic, transport, thermoelectric materials that allow us to produce electricity from lost heat that is released by different human activities (industry, automotive sector .....). In addition to heat recovery, the application of thermoelectric materials in the field of refrigeration would allow the manufacture of silent devices and free of polluting gases. [1] This thermoelectric conversion does not use mechanical systems, as complex as fragile and expensive maintenance. It is non-polluting unlike batteries because thermoelectric generators have an almost unlimited life. As such, thermoelectricity should emerge and play a role in future years by valuing huge amounts of lost energy and contributing to sustainable development or integrating with other emerging technologies.

We will look for new materials. Recent studies show that magnesium-type materials Mg2X (X = Si, Sn, Ge ...) have interesting thermoelectric properties for applications in high temperature electricity generation. Thus, the elements that make up this material are nontoxic and available elements (low cost) [2]. But, the performance of thermoelectric devices to this type of materials remains limited. To improve this, several ideas are proposed, among these ideas: the idea of forming solid solutions. For the subject of our memory, we will work on this idea, which allows us to reduce their thermal conductivity as a parameter of improvement. We apply different pressures on the thermoelectric solid solution Mg2Si1-xSnx electro thermal material, and then study its effects to take the appropriate pressure, which does not negatively affect the material, all calculation performed within the functional density theory (DFT).

In the first chapter, we present the basic principles of thermoelectricity and thermoelectric applications. Next, we highlight the thermoelectric parameters that optimize thermoelectric materials. Thus, we expose families of thermoelectric materials. In addition, we will expose motivations for them choice of studied in this work.

In The second chapter, we give an overview of the theoretical bases where we present the generalities related to non-relativistic quantum processing of a system composed of several particles and then we describe the Khon-Sham equations which give a new form of the equation from Schrödinger where we introduce the concept of electronic density functional (DFT). We introduce the approximations used to treat exchange and correlation potentials such as local density (LDA) and generalized gradient (GGA), we discuss the self-consistency procedure used in solving the Khon-Sham equations, and finally, to evaluate the transport coefficients, we use

the semi classical approach given by the solution of Boltzmann's equation in the relaxation time approximation

In the last chapter, results for the pressure effects on a thermoelectric material solid, using the method of augmented and linearized plane waves (FP-LAPW) implemented in the WIEN2K code, to determine the structural and electronic properties. The exchange and correlation potential (XC) is processed by the generalized gradient approximation (GGA) and the modified Beck Jonhson approximation (mBJ). And the calculation of transport properties by was conducted in the approach semi-classical BoltzTraP.

Bibliography

[1]: Boudemagh D : «Synthèse et Etude des Matériaux Thermoélectrique du Système $Mg_2Si_{1-x}Sn_x$. Physique», thèse de Doctorat, Université Joseph-Fourier - Grenoble I, 2010.
[2]:V. K. Zaitsev et al., « Highly effective Mg2Si1-xSnxthermoelectrics », Physical Review B, vol. 74, n°.4, p. 045207, 2006.

-.

Chapter I: generality about thermoelectricity

I. Thermoelectricity:

I.1 Introduction:

The effect of electricity due to heat is called thermo – electric effect. In thermoelectric phenomenon heat energy is converted into electric energy and vise-versa. It may be reversible and irreversible. Current produces heat as it passes through the conductor; this effect is called Joule's effect. Joule's effect is irreversible, meaning even if we change the direction of current flow in the conductor heat is always produced and that heat cannot be transformed into electric energy. However, we can produce electricity in a thermocouple just be heating of its one end and cooling the other one. Three different types of thermoelectric phenomena are being discussed here.

I.2 Historical:

A summary of the historical developments of thermoelectricity is presented below:

• **1821:** The German physicist Thomas Johann Seebeck discovers the first thermoelectric effect. He noticed that a metal needle is deflected when it is placed between two conductors of different nature linked at their end by junctions and that one of the junctions is maintained at a higher temperature than the other.

• This effect was interpreted as an appearance of a magnetic field and even served to explain the Earth's magnetic field. It was only later that it was shown that this phenomenon was explained by the appearance of an electric current between the cold and hot junctions.

• **1825:** Oersted gives the right explanation. He realizes that in reality, the temperature difference creates a potential difference which, if the circuit is closed allows the passage of the current and therefore induces a magnetic field

• **1834:** The French physicist Jean Peltier discovers the second thermoelectric effect, which is in fact the inverse phenomenon of the Seebeck effect either: if we apply a current to a metallic solid we observe a heat displacement of a face to the other. Here again the explanations provided by Peltier are incorrect.

• **1838:** Heinrich Lenz explains the findings of Peltier. If an electric current is passed through a circuit designed with two different materials and whose connections are at the same temperature, the heat is absorbed at one junction and returned to the other. This demonstration was carried out using the thermoelectric couple antimony / bismuth. The junction of these two metal wires is placed in a drop of water: when the current passes in one direction the drop of water freezes, when the current passes in the other direction, the ice melts.

• **1851:** William Thomson (Lord Kelvin) connects the Seebeck and Peltier effects. A material subjected to a thermal gradient and traversed by an electric current, exchanges heat with the

external environment. Conversely, an electric current is generated by a material subjected to a thermal gradient and traversed by a heat flow.

• **1865:** Robert Bunsen and Joseph Stefan show that semiconductors also give rise to the Seebeck effect with a much higher efficiency than those obtained with metals.

• **1909:** The German scientist Edmund Altenkirch performs for the first time the satisfactory calculation of the properties of thermoelectric circuits.[1]

• **1910:** Edmund Altenkirch suggested the concept of the merit factor. He showed that good thermoelectric materials should have a high Seebeck coefficient, high electrical conductivity and low thermal conductivity.

• **1949:** Abram Ioffe proposed that doped semiconductor materials are the best candidates for being thermoelectric materials.

• **1950:** Abraham Ioffe discovers that doped semiconductors have a higher thermoelectric effect than other materials.

• **1954:** Julien Goldsmid was the first to identify Bismuth Telluride as a material for thermoelectric refrigeration and showed that thermoelectric coolers could reach zero degrees Celsius

• **1990:** Regain of interest for thermoelectricity due to environmental concerns.

• **1995:** Glenn Slack introduced new criteria for selecting a good thermoelectric material and developed the concept of "Phonon Glass Electron Crystal". This material had to possess the electrical properties of a Crystal and the thermal properties of a glass.

The thermoelectric effect is a physical phenomenon characteristic of certain materials contributing to the conversion of energy. A thermoelectric material can directly convert heat into electricity (generation) or move calories by applying an electric current (refrigeration),Thus the thermal energy can be transformed into electrical energy and vice versa.[2]

I.2.1 Seeback effect:

The phenomenon of generation of an electric current in a thermo - couple due to a temperature difference at its two junctions is known as thermoelectric effect or Seeback effect. A thermo couple is a pair of wires of different materials whose ends have joined to form two junctions. When one junction is kept hot and the other cold, a current begins to flow through couple. This current is called thermoelectric current and the emf (electromotive force) due to which this current flow is called thermo emf. Thermo emf is the result of temperature difference between two ends of thermos couple. Due to different electronic concentration of the materials, there exists a contact potential at each junction, as shown in Figure I.1. [3]

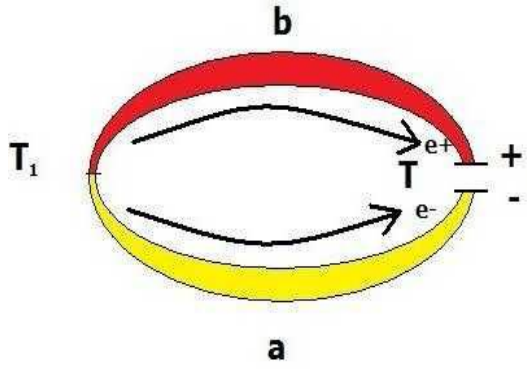

Figure I. 1: Illustration of the Seebeck effect.

By experimenting on the different sets of thermocouple Seeback listed the thermocouple series of different elements as –

Sb, Fe, Zn, Ag, Au, Cr, Sn, **Pb**, Hg, Mn, Cu, Co, Ni, Bi

Thermo-ve 0 Thermo+ve

I.2.2 Peltier effect:

The phenomenon of absorption or evolution of heat at the junctions of a thermocouple when current is passing through it is called Peltier effect. The absorption or evolution of heat depends upon the direction of flow of current, i.e. it is a reversible effect.

When two different metals are joined, contact potential is established at the junctions. This means one metal will be at higher potential than the other. In b – a thermocouple, a will be at higher potential than b. Therefore, when current flows from a to b at the junction a, energy has to be given out (evolved) at the junction a. Hence the junction a becomes hot. On the other hand, at the junction b, current flows from b to a, energy is to be absorbed by current and the junction b becomes cold, as shown in Figure I.2. [3]

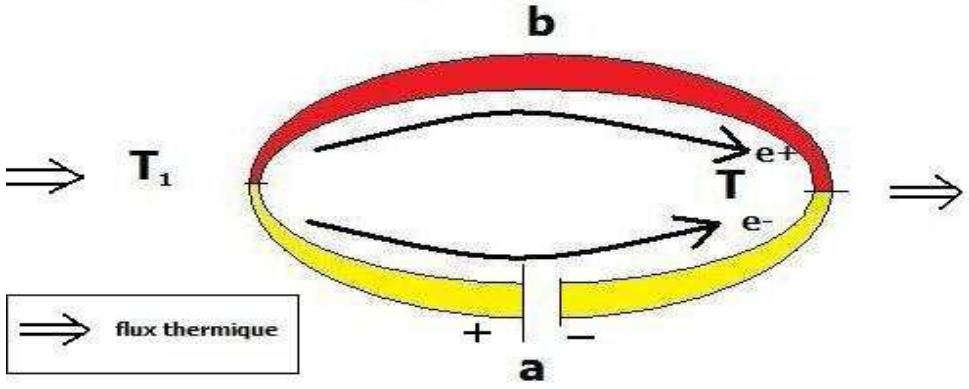

Figure I. 2 : Illustration of the Peltier effect.

I.2.3 Thomson effect:

The phenomenon of evolution or absorption of heat along the length of a conductor on passing a current through it, when different portions of the conductor are kept at different temperatures is known as Thomson's effect. It is observed that in copper, silver, zinc etc. when current is passed

from its hotter end to the colder end, the heat is evolved and the wire will become hot. On the other hand, if current is passed from colder end to its hotter end, heat will be absorbed and the wire will become cold. It is because the hotter end of such metal is at higher potential. This effect is known as +ve Thomson effect. In case of Iron, cobalt, nickel etc. when current is passed from hotter end to the colder end, heat is absorbed. It is because hotter end of iron is at lower potential. This effect is known as – ve Thomson effect, as shown in Figure I.3. [3]

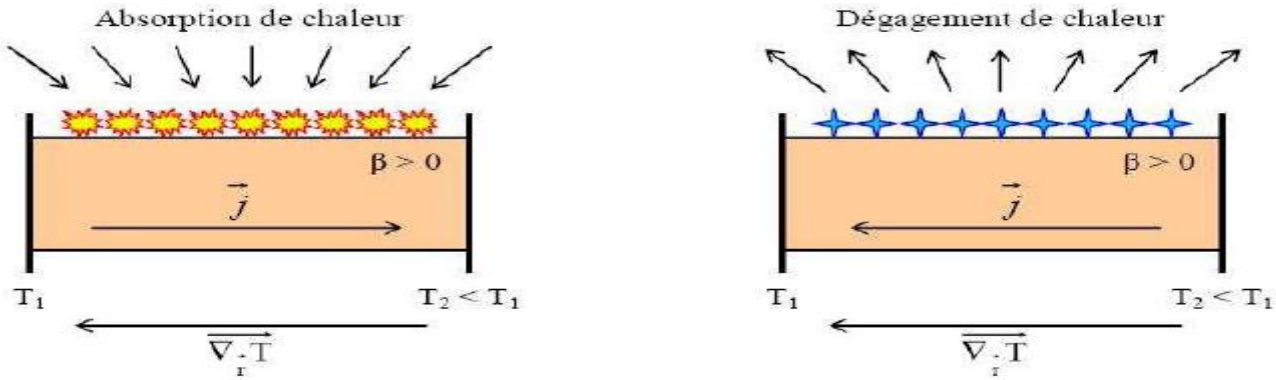

Figure I. 3 : Illustration of the Thomson effect.

Remarque$_1$:

Conversely, an electric current is generated if the material is subjected to a temperature gradient and a heat flux.

This effect is different from the Peltier and Seebeck effects. The latter exists for a single material and does not require a junction.

I.3 Thermoelectric coefficients:

If current is flowing and there is a temperature gradient, there is also heat generation or absorption within each segment of the thermocouple because α is temperature dependent. The gradient of the heat flux is given by

$$\frac{dQ}{dS}=\tau I\frac{dT}{dS} \quad \text{..... (I.1)}$$

Where S is a spatial coordinate.

It is useful that both τ and π can be obtained from α, which is easily measured. Experiments have confirmed the relationships derived by Kelvin:

$$\tau_a-\tau_b=T\frac{d\alpha_{ab}}{dT} \quad \text{..... (I.2)} \qquad \text{and} \qquad \pi_{ab}=\alpha_{ab}T \quad \text{.....(I.3)}$$

The last equation provides a fundamental link between thermoelectric cooling (π)

Thermoelectric cooling and power generation require joining two different materials. Therefore, it is π and α of couples that matter in practice. However, the absence of α for superconductors has made it possible to define an absolute α and π for individual materials. The α value for Pb-Nb_3Sn couples measured up to the critical temperature of the latter gave, α_{ab} for T < 18 K. Then, measurement of τ from 18 K to high temperatures yielded an absolute α for Pb, which became a reference material. The absolute thermoelectric coefficients also obey the Kelvin relationships[4]

$$\tau = \frac{d\alpha}{dT} \quad \text{..... (I.4)} \qquad \text{and} \qquad \pi = \alpha T \quad \text{..... (I.5)}$$

I.4 Optimization of thermoelectric materials:

Thermoelectric materials are characterized by three parameters:

- The Seebeck coefficient (V/K^{-1})
- Electrical conductivity ($\Omega^{-1}.m^{-1}$)
- Thermal conductivity (W/m.K)

A material with a large thermoelectric power factor, $S^2\sigma$, and therefore ZT, needs to have a large Seebeck coefficient (found in low carrier concentration semiconductors or insulators) and a large electrical conductivity (found in high carrier concentration metals).

The qualities of a thermoelectric material are measured by a dimensionless number, called merit factor ZT given by the relation:

$$ZT = TS^2 \frac{\sigma}{\lambda e + \lambda l} \quad \text{.....(I.6)}$$

The figure of merit $ZT = \sigma S^2 T/\lambda$ (α Seebeck coefficient, σ and λ the electrical and thermal conductivity, respectively) is an essential element of the efficiency of a thermoelectric material for applications, which convert heat to electricity or, conversely, electric current to cooling. From the expression of the power factor, σS^2, it was deduced that a highly degenerated semiconductor is necessary.

In order to reduce the lattice part of the thermal conductivity, various mechanisms, mainly related to the structure of the materials, were tested in new thermoelectric materials and had been the topics of different reviews. These include cage-like materials, effects of vacancies, solid solutions, complex structures (cluster, tunnel. . .), nano-structured systems. We plan to review structural aspects in the modern thermoelectric materials and to include results of the very recent years. [5]

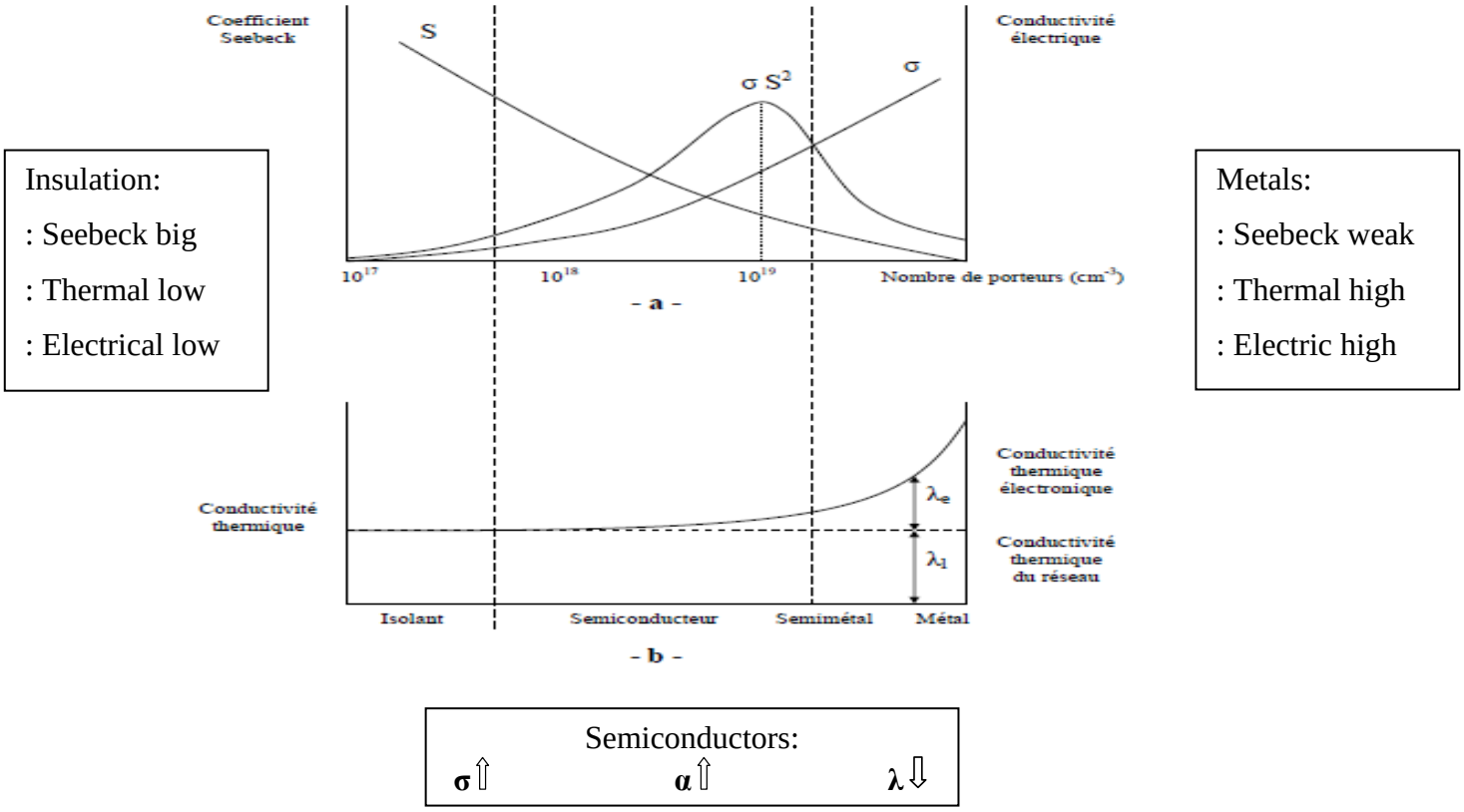

Figure I. 4 : Evolution of thermoelectric properties of materials according to Seebeck coefficient and electrical and thermal conductivities.

I.5 Conversion efficiency:

The optimization of the materials is needed to enhance their transport properties and maximize the figure of merit ($ZT=TS^2\frac{\sigma}{\lambda e+\lambda l}$):

With $\sigma = 1/\rho$ and λ the electrical and thermal conductivities, respectively. For cooling applications, the efficiency of the system is given by the coefficient of performance COP which, in an optimized system, is:

$$COP=\frac{\text{heat extractd from the cold side}}{supplied\ electrical\ power} \qquad COP_{max}=\frac{Q}{W}=\varepsilon_C\frac{\sqrt{1+Z_{AB}\frac{T_{ch}+T_{fr}}{2}}-\frac{T_{ch}}{Tfr}}{\sqrt{1+Z_{AB}\frac{T_{ch}+T_{fr}}{2}}+1} \quad \text{.....} \ \textbf{(I.7)}$$

Where εc is the coefficient of performance of Carnot:

$$\varepsilon_C=\frac{T_{fr}}{T_{ch}+T_{fr}} \quad \text{.....} \textbf{(I.8)}$$

For electricity generation, the maximum conversion efficiency is given by:

$$\eta=\frac{Power\ supplied\ to\ the\ load}{Absorbed\ heat\ at\ the\ hot\ end} \qquad \eta_{max}=\frac{W}{Q}=\eta c\frac{\sqrt{1+Z_{AB}\frac{T_{ch}+T_{fr}}{2}}-1}{\sqrt{1+Z_{AB}\frac{T_{ch}+T_{fr}}{2}}+\frac{T_{fr}}{T_{ch}}} \quad \text{.....} \ \textbf{(I.9)}$$

Where ηC is the Carnot yield characteristic of thermal machines:

$$\eta c=\frac{T_{ch}-T_{fr}}{T_{ch}} \quad \text{.....} \textbf{(I.10)}$$

Electrical conductivity:

By definition, is given, for a material of type n and of type p, by the respective formulas

$$\sigma=(q\times n\times \mu_a) \quad \text{.....}\textbf{(I.11)}$$
$$\sigma=(q\times p\times \mu_p) \quad \text{.....}\textbf{(I.12)}$$

With n and p the densities of carriers, q the carrier charge of a carrier and μ the mobility of these carriers.

Mobility can be expressed as:

$$\mu_{np}=\frac{q\times\tau_{np}}{m^*_{np}} \quad \text{.....}\textbf{(I.13)}$$

With τ_n, p the relaxation time of the carriers n and p and m^*_{np} their effective mass

Thermal Conductivity

Intuitively, a good thermal conductivity would prevent a large temperature gradient. However, the thermal conductivity includes mainly two components: an electronic contribution λe, due to the movement of carriers, and a lattice contribution via the phonons λ_L: $\lambda = \lambda e + \lambda_L$. The electronic part of the thermal conductivity is related to the electronic conductivity via the Wiedemann–Franz law:

$$\lambda_e=L_0\times\sigma\times T \quad \text{.....}\textbf{(I.14)}$$

With Lo the Lorentz factor. In metals, it is equal to the Lorentz number:

$L_0=\frac{1}{3}\left(\frac{\pi K_B}{e}\right)^2 = 2,\ 45\ \cdot\ 10^{-8}\ V^2.K^{-2}$, value generally used as a first approximation for the TE semiconductors. Replacing λ by its two components and with the Wiedemann– Franz, leads to:

$$ZT=\frac{\alpha^2}{L_0}\left(1+\frac{\lambda_1}{\lambda_0}\right)^{-1} \quad \text{.....} \textbf{(I.15)}$$

I.6 Generation of electricity and cooling:

Thermoelectric Power Generation:

Thermoelectric elements generate electrical power from heat based on the Seebeck effect. A basic thermoelectric generator consists of a p-type and n-type leg. In the figure below, the elementary configuration is presented. In practice a module utilizes a number of these p-type and n-type legs usually called couples and are connected thermally in parallel and electrically in a series.

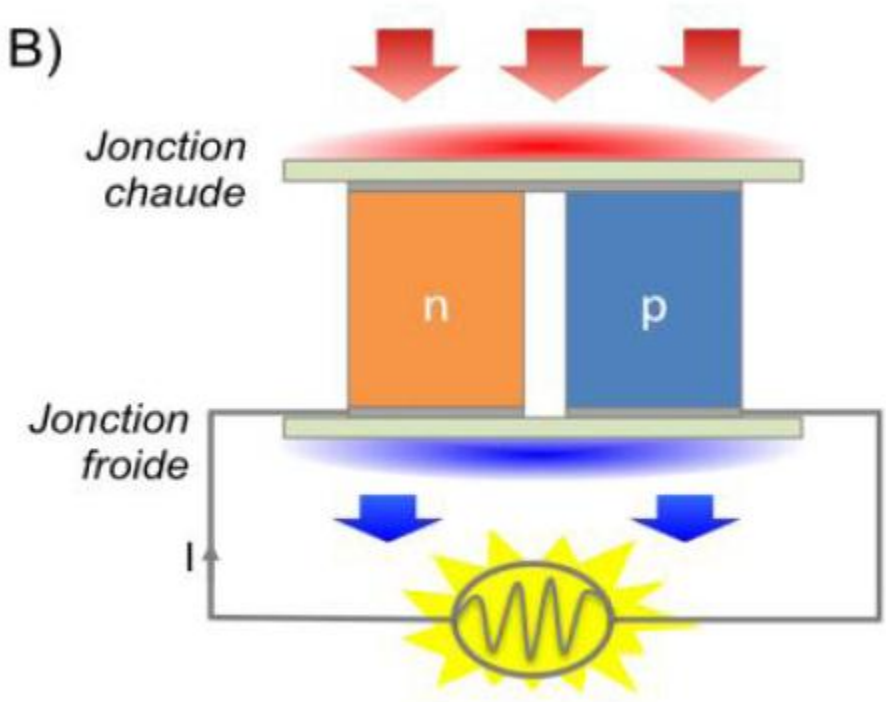

Figure I. 5 : The two element power generator utilizing the Seebeck effect.

From Figure 5, it is observed that heat flows through the device from the top of the setup and released from the opposite side. In n-type thermoelectric material, the majority of carriers are electrons. In p-type material the majority carriers are holes. Heat flows through the two p-type and n-type from the hot to the cold side of the device. If the device is connected to a circuit of a load resistor, the device creates a current in the circuit and acts like a power generator. The Seebeck voltage produces an electrical current I which is proportional to the temperature gradient between the hot and cold junctions ΔT.[5]

Thermoelectric Cooling:

As mentioned above, the Peltier effect is used for cooling. If a current is applied through the thermoelectric couple as shown in Figure 6, heat is pumped from the hot junction to the cold junction. The temperature of the cold junction will drop below ambient rapidly, provided that the heat is eliminated from the hot side. The temperature gradient will differ according to the amount of current applied to the device.[5]

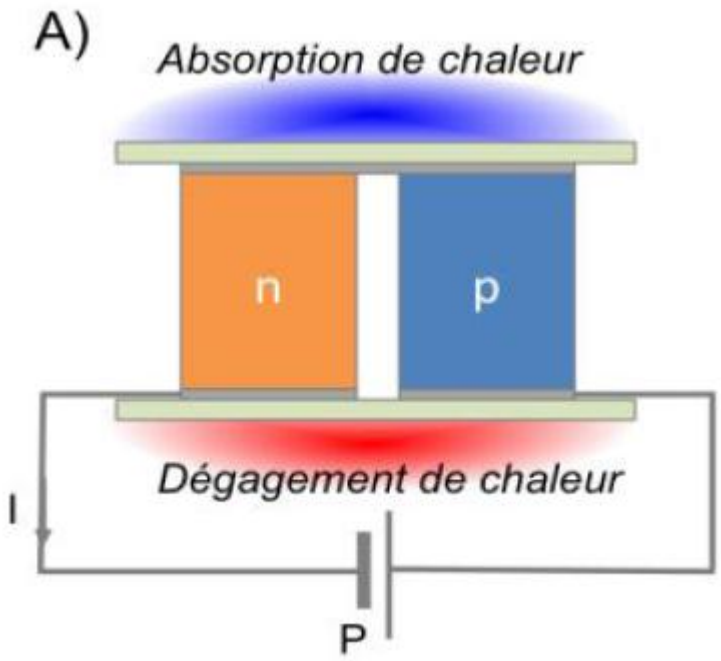

Figure I. 6 : Single-couple refrigerator utilizing the Peltier effect.

Thermoelectric generators (TEG) based on the principle described above have long been used for the generation of electrical power ranging from low power (microwatts) to high power (a few kilowatts), from ubiquitous heat sources. We can cite as an example:

(a) (b)

Figure I. 7 : Radio powered by thermoelectric module using the heat of a kerosene lamp (a), wood burning oven with integrated thermoelectric module for the production of electricity (Philips Research) (b).

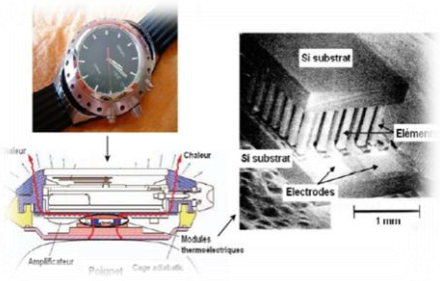

Figure I. 8: Seiko Thermic watch using the difference between the ambient temperature and that of the human body [6]

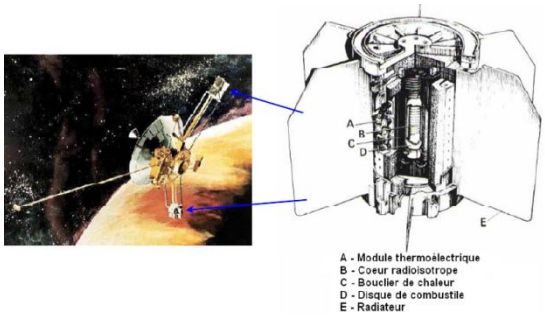

Figure I. 9: Pioneer 10 space probe powered by a thermoelectric radioisotope generator

Compared to conventional techniques, cooling by thermoelectric effect confers the same advantage as that of geneators, that is to say that of not using liquid or refrigerant gas, hence the Ecological interest of applications [6], [7] . due to their compactness, refrigerators cam be used for local cooling, Integrating the cooler near the component to be cooled. This leads to increased dynamic performance of the cooling system. currently, several types of devices based on thermoelectric modules are marketed for different areas of application: domestic (portable refrigerators, (Figure 11 a), automobile (locally seats, (Figure 11 b), and electronics (active and local cooling). Microprocessors) or optoelectronics (laser diodes (Figure 11 c)) [8].

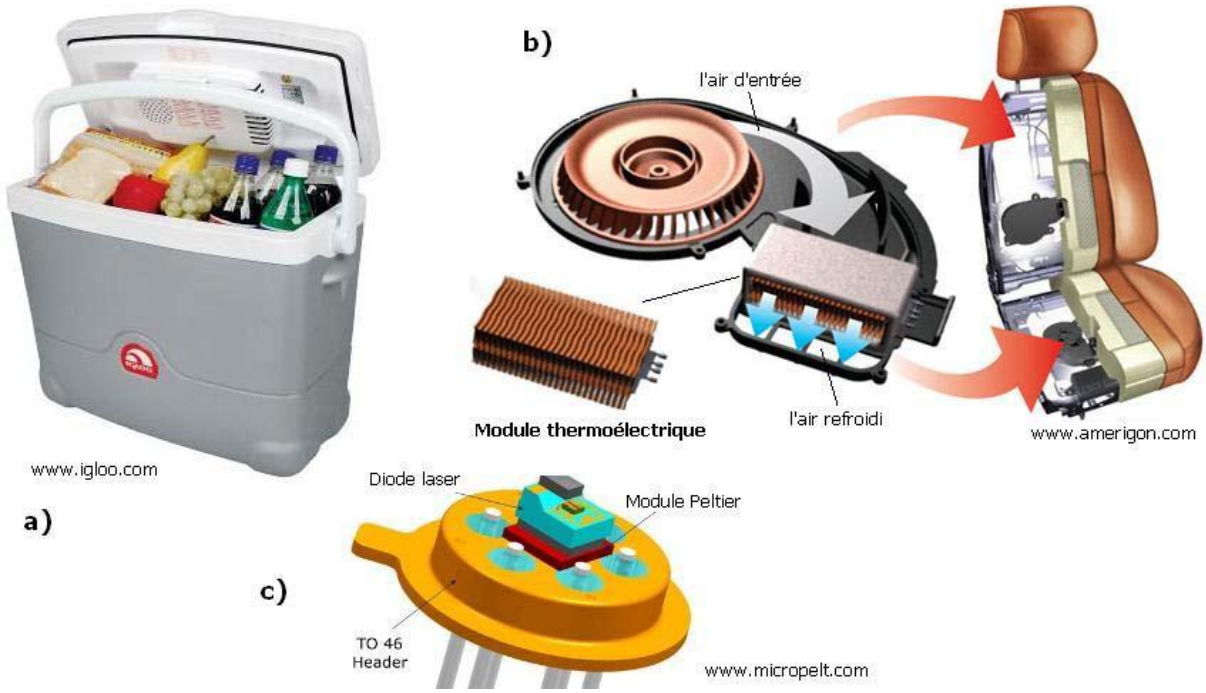

Figure I. 10: Cooling applications based on thermoelectric modules: (a) portable refrigerator, (b) car seat, and (c) laser diode.

I.6.1 Conventional materials:

From 1960, all actually used TE materials (see Table 1) were known and their performance, bound to a stagnant ZT to ~1, have not much changed up to 1990.

Thermoelectric materials have good thermoelectric properties only over restricted temperature ranges. We will present the different materials according to their range of use.[9]

	Bi–Sb	Bi_2Te_3–Sb_2Te_3	$(Bi,Sb)_2(Te, Sb)_3$	PbTe	Te–Ag–Ge–Sb	SiGe
Type	**n**	**n,p**	**n,p**	**n**	**p**	**n,p**
T_u (K)	**200**	**< 300**	**~300−400**	**700**	**750**	**1.000**
ZT at T_u	**1.1 (H)**	**0.8**	**0.9**	**0.8**	**1.1**	**0.6**

Tableau I. 1: ZT of conventional materials at their optimal temperature of use Tu.

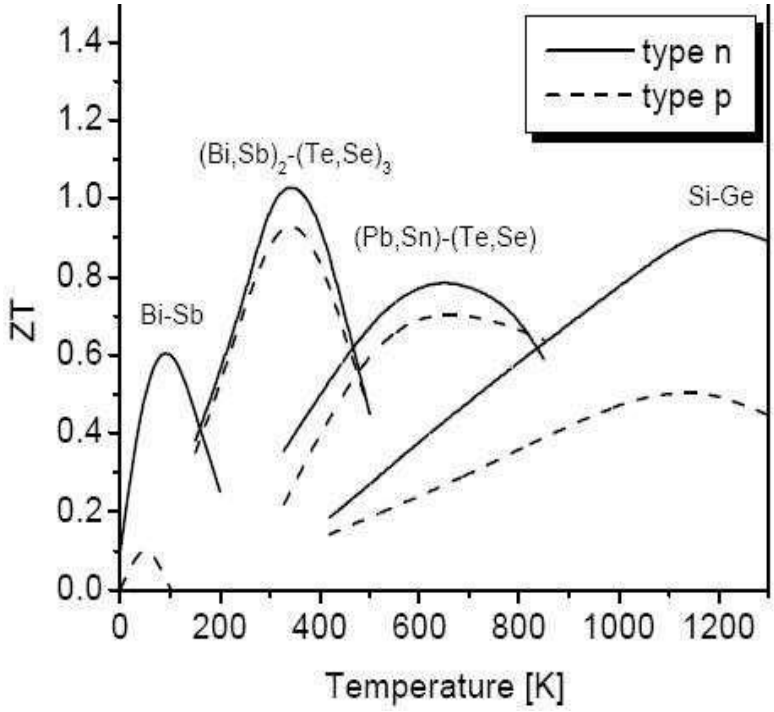

Figure I. 11 : Variation of the merit factor as a function of temperature.

I.6.2 New materials:

Thermoelectric materials currently exhibit maximum ZT merit factors around the unit, which leads to conversion efficiencies of about 5-7%. These values remain low compared to the 30-45% efficiency of modern internal combustion diesel engines [10], that of about 30% for domestic refrigerator. For thermoelectric devices to become competitive, the ZT merit factor must be greater than 1.5 for power generation applications , and from 2 to 4 for cooling applications[11]. So we need to optimize the merit factor, the advantage of this optimization is that thermodynamics imposes no limit on this factor, but interdependence of thermoelectric properties (S, σ, λ_e, λ_p) is a big obstacle. The ideal would be to be able to decouple the parameters S, σ, and λ in order to intervene independently on each one of them.

This would increase the power factor ($S^2\sigma$) and decrease the thermal conductivity, especially the λ_{ph} phonon component, and thus improve the merit factor[12] . For this purpose (optimization of ZT) there are two approaches:

- **Classical approaches:**

They are based on theoretical foundations well known to date; these approaches are taken up in current research. Optimization by these approaches is based on strategies [5] to increase the power factor ($S^2\sigma$) by:

- Optimization of the charge concentration by doping.
- The use of dopants that can introduce energy levels close to the resonant levels with the Fermi level of the material.

To reduce the thermal conductivity by:

- The formation of compounds whose point defects are effective for phonon scattering.
- The use of materials with a complex crystal structure or constituents that do not have a well-defined position in the crystal lattice.
- The use of materials composed of elements of great atomic mass.

➢ **New approaches:**

It allows decoupling the three parameters: S, σ and λ. The idea is to introduce nanometric constituents or to use nano-structured materials (whose dimensions at <~ 100 nm). The goal of this approach is:

- To increase the density of electronic states near the Fermi level by quantum confinement of the charges (thus increasing the Seebeck coefficient).
- To create many interfaces, effective for phonon scattering and thus reduce the thermal conductivity of the network.

I.6.2.1 Single-Phase Materials :

Skutterudites:

Skutterudites are a highly promising and deeply researched class of compounds. They crystallize in the $CoAs_3$-type structure with the cubic space group $Im\bar{3}$. The structure is composed of eight corner-shared XY6 (X=Co, Rh, Ir; Y=P, As, Sb) octahedra. In fact, the $CoAs_3$-structure type is a severely distorted version of the perovskite AB_3 type structure. Figure 13 a and b show that the linked octahedral [13]

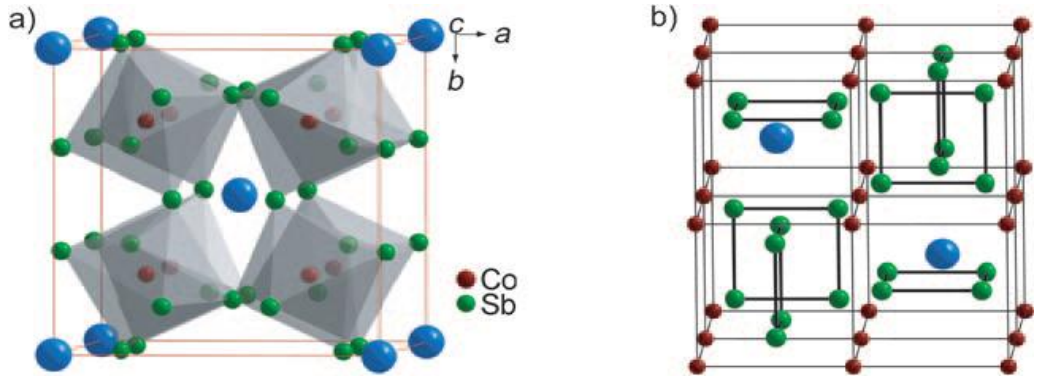

Figure I. 12: Two model structures of the skutterudite, CoSb3 ; the void cages are filled with blue spheres for clarity. a) The unit cell of skutterudite structure. The transition metals (Co) are at the center of octahedra formed by pnicogen atoms (Sb). b) The model shifted by the fractional coordinates 0,25; 0,25; 0,25 from the unit cell. The Co atomsare connected for clarity. The only chemical bonds in this model are those of the Sb squares.

Clathrates:

The clathrates are generally low-thermal conductivity compounds with open frameworks composed of tetrahedrally coordinate Al, Ga, Si, Ge, or Sn. The framework has cages that can incorporate large electropositive atoms. There are two main types of structure the so-called Type I and Type II with the former being more common. The Type I structure can be represented by

the general formula $X_2Y_6E_{46}$ (Figure14a, Na_8Si_{46} for example), where X and Y are "guest" atoms encapsulated in two different polyhedral cages E_{20} and E_{24}, while E represents tetrahedrally coordinate framework atoms. The Type II structure is composed of E_{20} and E_{28} cages. [13]

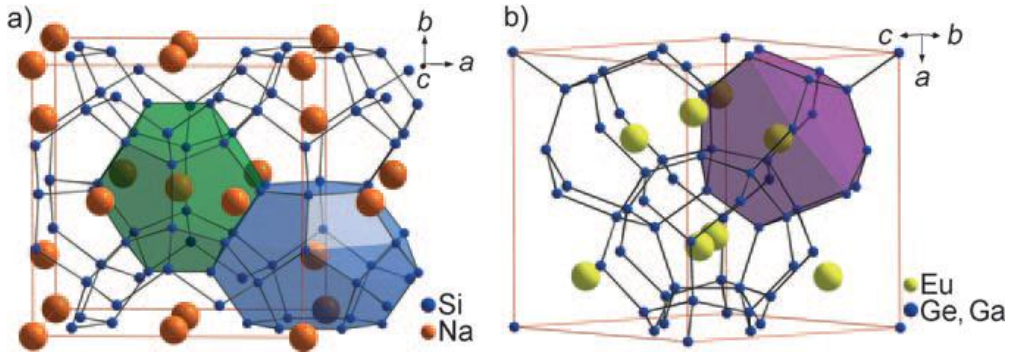

Figure I. 13: a) Crystal structure of the Type I clathrate, Na_8Si_{46}. Framework composed of Si atoms (blue) and two different cages with guest Na atoms, the tetrakaidecahedral cage (blue) and the pentagonal dodecahedral cage (green). b) Crystal structu of the Type VII

Half-Heusler Intermetallic Compounds:

Another class of compounds of considerable interest as potential thermoelectric materials for high-temperature applications are the half-Heusler (HH) intermetallic compounds formulated as MNiSn (M=Ti, Hf, Zr). HH phases have the MgAgAs crystal structure which consists of three filled interpenetrating fcc sublattices and one vacant sub lattice. The general formula is XYZ, where X and Y are transition metals and Z is main-group element .They are relatively easily synthesized. Another advantage of these compounds is their high melting points of 1100–1300 C as well as their chemical stability with essentially zero sublimation at temperatures near 1000 C. Figure 15 shows the unit cell [13]

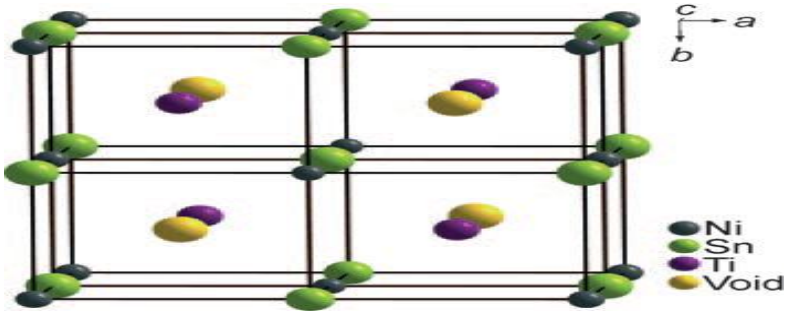

Figure I. 14: Crystal structure of the half-Heusler, TiNiSn, in a unit cell of cubic structure (a=5.9210A˚). For clarity the void space is filled with void atoms in yellow

b-Zn_4Sb_3:

b-Zn_4Sb_3 is a promising p-type compound at moderate temperatures which exhibits exceptionally low thermal conductivity . The crystal structure of β-Zn_4Sb_3 is hwon in Figure16, and has one Zn site and two independent Sb sites [13]

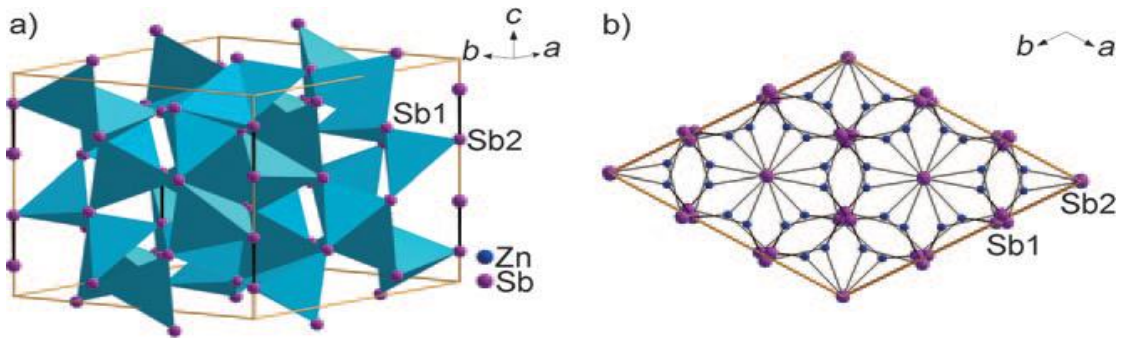

Figure I. 15: The crystal structure of β-Zn4Sb3 consists of a) three-dimen- sional corner-sharing tetrahedral of [ZnSb4] units and b) Sb2 dimmers which form in the octahedral holes within the distorted hexagonal Sb1 channels (view down to the c axis).

The Zintl Phase $Yb_{14}MnSb_{11}$:

$Yb_{14}MnSb_{11}$ has emerged recently as a promising intermetallic thermoelectric material for very high temperatures. The compound belongs to the Zintl family, $A_{14}MPn_{11}$, where A is an alkaline-earth or rare-earth metal, M is a transition or main-group metal, and Pn is a pnicogen, several members of which have been extensively studied for their magnetic properties. The Yb analogue appears to be an excellent p type thermoelectric material. Figure 17 shows the cubic structure of $Yb_{14}MnSb_{11}$ which crystallizes in the complex structure of $Ca_{14}AlSb_{11}$. It consists of one $[AlSb_4]$ tetrahedron, one $[Sb_3]$ polyatomic anion, four Sb^{3-} anions situated between $[AlSb_4]$ and $[Sb_3]$ units, and $14Ca^{2+}$ per formula. $Yb_{14}MnSb_{11}$ is considered to be a valence precise semiconductor based on the classical Zintl concept in which the strongly electropositive Yb atoms donate electrons to Sb atoms in the structure. In reality, the material exhibits weakly metallic or semi metallic behavior as a function of temperature. [13]

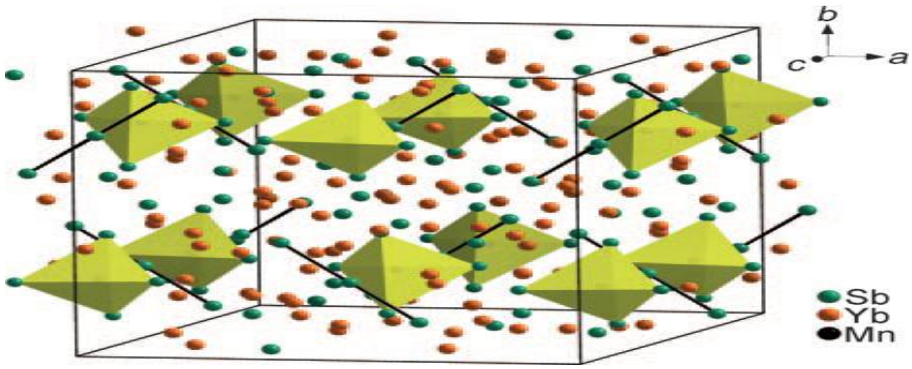

Figure I. 16: The cubic crystal structure of $Yb_{14}MnSb_{11}$ consists of one $[MnSb_4]$ tetrahedral unit (yellow), one $[Sb_3]$ ion (centers linked by black lines), four Sb_3- ions situated between the $[MnSb_4]$ and $[Sb_3]$ units, and 14 Yb2+ ions per formula.

I.6.2.2 Nanostructure materials:

In 2004, P.X.Zhang shows that thin films show performance thermoelectric properties significantly (up to a factor of 3) than those obtained in solid materials. On the other hand, the thermoelectric coefficients are independent between them .[14]The other interest of thin films is

the reduction of the size of the systems and their integration in thermoelectric Microsystems while retaining the thermoelectric properties of massive materials (figure I.18).

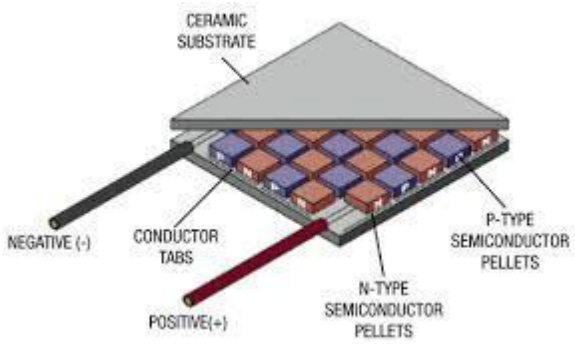

Figure I. 17 : Reducing the size of a cooling generator.

I.7 The choice of Mg2Si1-xSnx :

I.8 Introduction:

Despite the discovery of the 2-3 merit factor materials, the commercial modules for thermoelectric technologies are based on conventional materials, i.e. compounds based on Bi-Te, Pb-Te or Si-Ge. In addition the merit factor, these materials must meet the requirements in terms of thermal and chemical stability throughout the intended temperature range, availability of natural resources of the constituent elements (problem cost), toxicity and harmfulness. From this point of view, the basic compositions Bi-Te and Pb-Te are unfavorable because Pb is a very toxic and forbidden element in several countries. It is the same for Bi and Te. So, we will look for a material that meets these needs.

In 2006, V. K. Zaitsev et al. Studied $Mg_2Si_{1-x}Sn_x$ type compounds. they have obtained a merit factor of 1.1 in the temperature range of 700 to 870 K, which attracted much attention and re-launched important research around these materials .[15] There is further work showing that solid solutions of $Mg_2Si_{1-x}Sn_x$ and their parent compounds (Mg_2Si and Mg_2Sn) are considered promising thermoelectric materials [16] [17]Their interest lies not only in the merit factor close to that of conventional materials, but also in the availability (therefore low cost) and non-toxicity of the constituent elements.

Figures I.19 and I.20 represent respectively: the price in euro's per kilogram of all the natural and pure chemical elements according to their abundances in ppm in the earth's crust, and the non-toxicity of these elements. We note that the elements Mg, Si and Sn are of ecological interest, economic in addition to their abundance in nature.

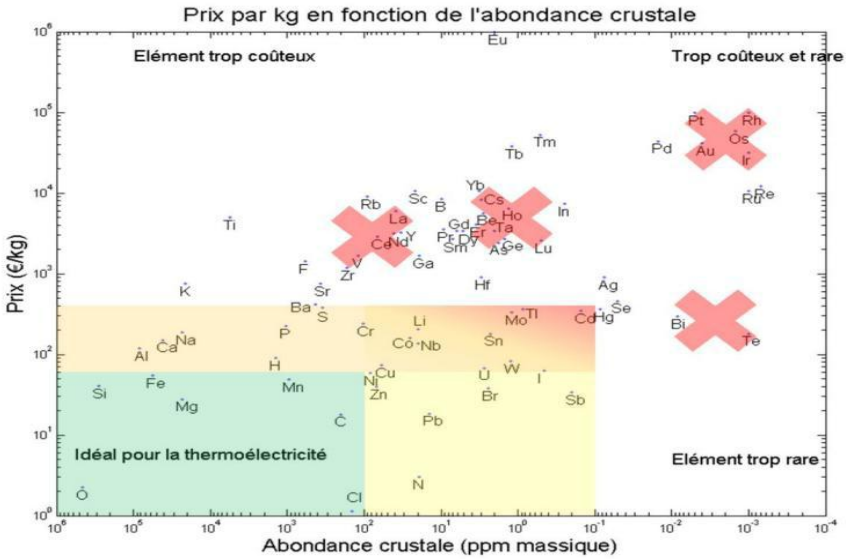

Figure I. 18 : Price in euro's per kilogram of pure chemical elements in function

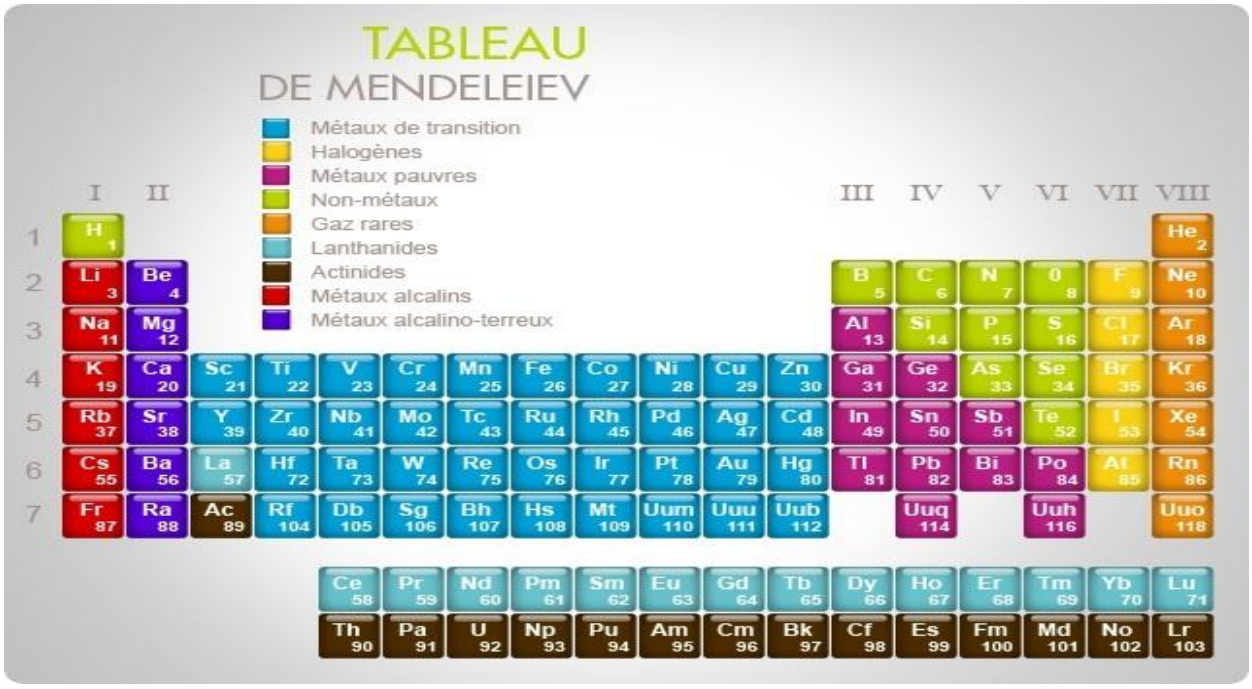

Figure I. 19 : Periodic table

I.9 The compounds Mg_2X (X=Si or Sn):

During the years 1960, the Ioff´e Institute showed that the compounds Mg2X (X=Si, or Sn) are semiconductors with a band structure which should favor TE properties. Various substitutions have been tested and the best results have been obtained when the mass difference between elements is the highest, i.e., with Si and Sn[18]. A ZT of 1.1 has then been found at 800 K, a better value than with n-type Si-Ge [19]

The inter metallic compounds Mg2X (X = Si or Sn) crystallize generally with the cubic face-centered structure (CaF2 fluorite type) of Fm3m space group (Figure 21). The cell parameter

increases with the atomic radius of the atoms B, and its value is of ~ 6.38 Å for Mg2Si, ~ 6.76 Å for Mg2Sn [20] .

We recall that the compounds of $Mg_2Si_{1-x}Sn_x$ (x = 0, 0.25, 0.5, 0.75, 1) crystallize in the anti-fluorite type structure: the atoms Si (Sn) takes the position (0; 0; 0) and the atom Mg positions in (1/4, 1/4, 1/4), In Figure I.21.

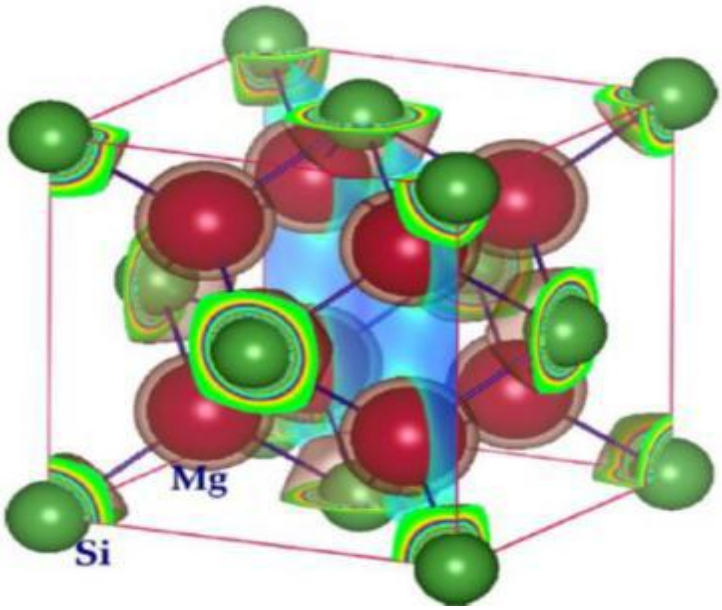

Figure I. 20 : Crystal structure of the compound Mg2Si (Mg2Sn). Mg red atoms occupy the tetrahedral sites and the green Si (Sn) atoms occupy the CFC sites. Figure from the publication

Chapter II. Ab-initio methods

Chapter III. Results and Discussions

III. Results and Discussions:

III.1 Introduction:

This chapter is aimed to give more insiglut on the not yet explored pressure effects on the structural, electronic and transport properties of the solid solution $Mg_2Si_{1-x}Sn_x$. After, we will give a general description on the calculation detail. We will present the results and discuss them in an analytical and comparative way (with other works).

III.2 The calculation detail:

All of our calculations are based on the DFT (Wien 2k -DFT) which is included in the Wien 2k[2] code and Boltzmann approaches (semi-classical approach), made by BoltzTraP[1]. The calculations were carried out using the FP-LAPW method (all electrons). For the exchange potential and correlation, we used GGA approximations (Perdew-Burke-Ernzerhof "PBE" [2]) and the mBJ potential (as correction) for a better estimation of the gap value for the $Mg_2Si_{1-x}Sn_x$ system (especially for the Mg2Sn) [3], the unit cell is divided into two regions, the first consists of non-overlapping spheres centered on each atom of radius RMT, the second is the interstitial region (The RMTKmax parameter determines the size of the base in the interstitial region where RMT is the smallest radius Muffin -Tin and Kmax the norm of the largest wave vector used for the plane-wave development of eigenfunctions). Radiation values were set at RTM (Mg) = 2 a.u, RMT (Si) = 2 a.u and RMT (Sn) = 2.4 a.u. Structural optimization involves determining the ground state. The iteration process is repeated until the total energy is stable withing 10^{-5}Ry. The integration of K into the Brillouin zone is performed using the Monkhorst and Pack approach [4] leading to 156 K-special points for $Mg_2Si_{1-x}Sn_x$ k-point compounds set (8 × 8 × 8) for
(x = 0.25, 0.5, 0.75) and (20 × 20 × 20) for (x = 0 and 1) calculation.
This calculation is under different pressures (P=5Gpa; P=10Gpa and P=15Gpa).

III.3 Structural properties:

For a good simulation of the physical properties we must first optimize the structure, it allows to find the cell parameter and the reduced coordinates that correspond to the minimum energy. We recall that the compounds of $Mg_2Si_{1-x}Sn_x$ (x = 0, 0.25, 0.5, 0.75, 1) crystallize in the anti-fluorite type structure: the atoms Si (Sn) takes the position (0; 0; 0) and the atom Mg positions in (1/4, 1/4, 1/4). In Figures III.1, we present the crystal structures of the compounds $Mg_2Si_{1-x}Snx$ (x = 0, 0.25, 0.5, 0.75, 1) .We present three structures: Mg_2Sn (the equivalent of Mg_2Si), $Mg_2Si_{0.25}Sn_{0.75}$ (the equivalent of $Mg_2Si_{0.75}Sn_{0.25}$) and $Mg_2Si_{0.5}Sn_{0.5}$.

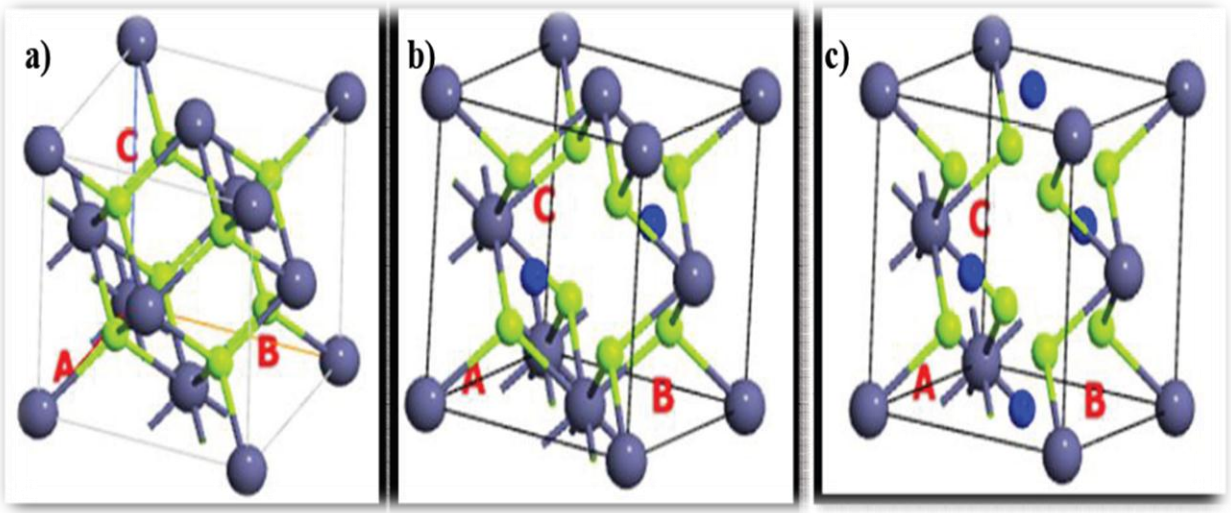

Figure III.1: The crystalline structure of the compounds Mg_2Sn (Si) a), $Mg_2Si_{0.25}Sn_{0.75}$ ($Si_{0.75}Sn_{0.25}$) b) and $Mg_2Si_{0.5}Sn_{0.5}$ c). The atoms of Sn in gray, Si in blue and Mg in green.

The values of the optimized cell parameters are reported in Table 1 with the results of other works (Theo and exp).the obtained results agree well with their available experimental counterpart. Actually, the maximum relative deviations of the optimized unit cell parameter at 0Gpa for Mg_2Sn (x=1) is about 0.59%. the good agreement between our results and the experimental values confirm the ratability of the calculation methodology adopted here , and give confidant on the subsequent results for the pressure effete our the transport properties , from table III.1, it can be clearly seen that the optimized lattice parameter a decreases with increasing pressure; this simple trend has been also reported in other work.

$Mg_2Si_{1-x}Sn_x$		x=0	x=0.25	x=0.5	x=0.75	x=1
Our calc (A°)	P=0Gpa	6,36	6,48	6,60	6,70	6,80
	P=5Gpa	6,18	6,30	6,40	6,50	6,55
	P=10Gpa	6,05	6,17	6,20	6,35	6,35
	P=15Gpa	5,94	6,07	6,15	6,24	6,18
Other calc P=0Gpa		6,36[5]	-	6,594 [5]	-	6,80[5]
Exp P=0Gpa		6,359 [6]	-	-	-	6,760[6]
Deviations (%)		0.015%				0.59%

Table III.2 : The lattice parameter of the compounds Mg2Si1-xSnx en comparison with theoretical and experimental data (at 0 GPa)

atom	Atomic number	Valence state	R_{MT}
Mg	12	$Mg:3s^2$	2
Si	14	$Si: 3s^2\ 3p^2$	2
Sn	50	$Sn:4s^{10}5S^25p^2$	2,4

Table III.3 : Valence state and the RMT rays of the atom Mg, Si, Sn.

Space group name Mg_2Si: F m -3 m; Mg_2Sn: F d -3 m

It should be noted that the equilibrium lattice parameters are calculated as the total energy Vs volume function, using the Murnaghan equation given by:

The Murnaghan equation:

$$E=E_0 + [B' \times \frac{V}{B'} \times \left(\frac{1}{B'-1}\right) \times (\frac{V_0}{V})^{B'} + 1 - \frac{B \times V_0}{(B'-1)}] \quad \text{.....(III.1)}$$

Pressure:

$$P= \frac{B}{B'}((\frac{V_0}{V})^{B'-1}) \quad \text{.....(III.2)}$$

Volume:

$$V^{(-B')} = V_0^{-B'} * \frac{B'}{B}(P+\frac{B}{B'}) \quad \text{..... (III.3)}$$

Where (V is the volume and E the equilibrium energy, B the compression modulus has the equilibrium and B' is its derivative with respect to the pressure).

Figure III.2 shows the total energies as a function of volume and after using fitting in the Origin code.

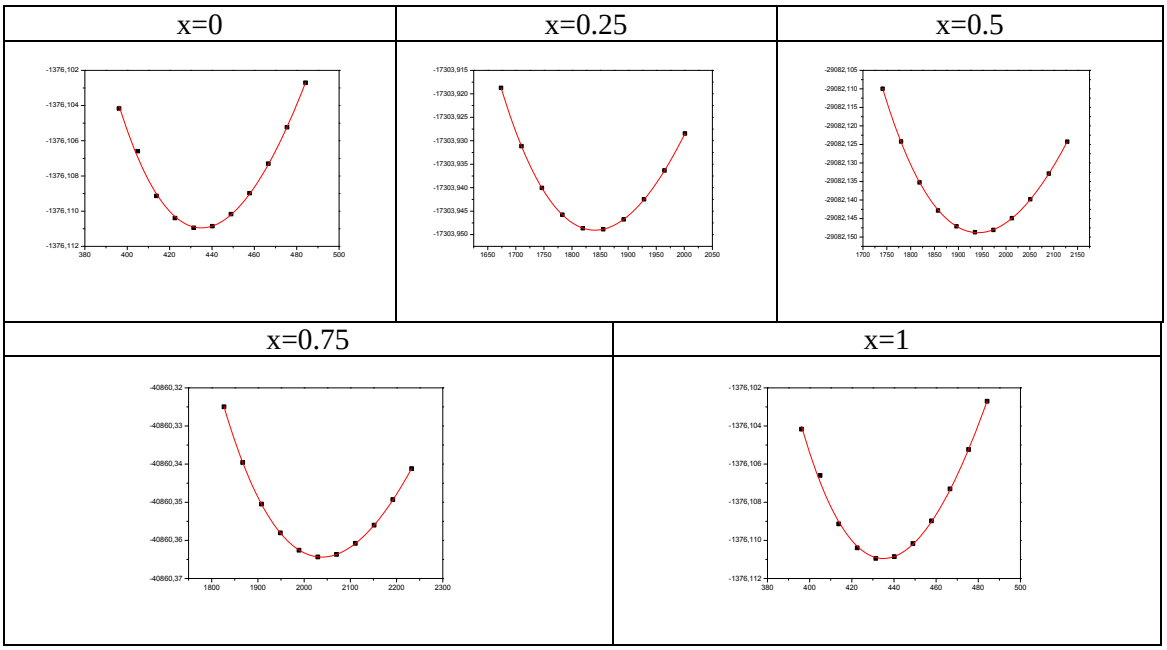

Figure III.2: Representation of total energy as a function of volume for states.

III.4 Electronic properties:

The electronic structure calculations were performed using density functional theory (DFT) with the Perdew-Burke-Ernzerhof (PBE) generalized gradient approximation (GGA) as implemented in (Wien 2k) code. To obtain a more accurate band gap For the GGA calculation, the mBJ [6] approximation was also used. The latter is used to improve the results of the energy gaps, to be comparable to the experiment. The network parameters used in the calculations are those optimized by the self-consistent calculation carried out previously. The Linearized projector-augmented wave (FP-LPAW) method was adopted with $2p^6\ 3s^2$ and $3s^2\ 3p^2$ as valence electrons for the Mg and Si atoms, respectively.

III.4.1 Band structures:

The most significant description of the energy surfaces offered to electrons occurs in the reciprocal space or space of the wave vectors k. This description is generally simplified in the form of a diagram which draws the variations of the energy E as a function of k according to points of high symmetry in the first Brillouin zone, called the band structure. For our compounds, we note well that the compounds Mg_2Si and Mg_2Sn have indirect gap ($\Gamma \rightarrow X$) and the compounds $Mg_2Si_{1-x}Sn_x$ (x=0.25, 0.5, 0.75), have direct gap ($\Gamma \rightarrow \Gamma$) for pressure (P = 5 Gpa; 10 Gpa and 15Gpa) in the compounds $Mg_2Si_{1-x}Sn_x$ (x = 0.25, 0.5, 0.75), the point Γ is the site which corresponds to the maximum of the valence band BV and the minimum of the conduction band BC. In Mg_2Si (Sn), the maximum of BV and the minimum of BC are respectively in points Γ and X respectively. This energy separation (gap energy) of each composition of our work is summarized in Table 3, 4 and 5.

In addition, the use of Beck Jonhson's modified potential (mBJ) as a correction of the terms of exchange and correlation allowed us to obtain energy gaps in good agreement with the experimental results. Thus, these results show a considerable improvement over those found using GGA(PBE) approximations. as shown in **Figure III.(3,4,5)**

Pressure effects on Energy gap a decrease with increasing pressure (Eg↓)

Remarking

-The **indirect** gap of which the minimum of the conduction band and the maximum of the valence band are located at different points of the K space.

-The **direct** gap for which these extreme are located at the same point of the K space (against the Brillouin Zone, in K = 0).

-In the direct gap semiconductor, the central minimum of the conduction band corresponds to electrons of low effective mass and therefore very mobile. On the other hand, that with an indirect gap, their conduction band corresponds to large electron effective mass, thus having a low mobility.

we can conclude that the gap value of all the concentrations $Mg_2Si_{1-x}Sn_x$ system decreases with the increase of the pressure, which will influence the transport properties so as to improve them, except for Mg_2Sn where it can be seen that There is an increase in the gap value up to 5GPa pressure, and then after 5GPa they decreasing (more than 10GPa), which also has been seen in previous works for the Mg_2Sn compound.

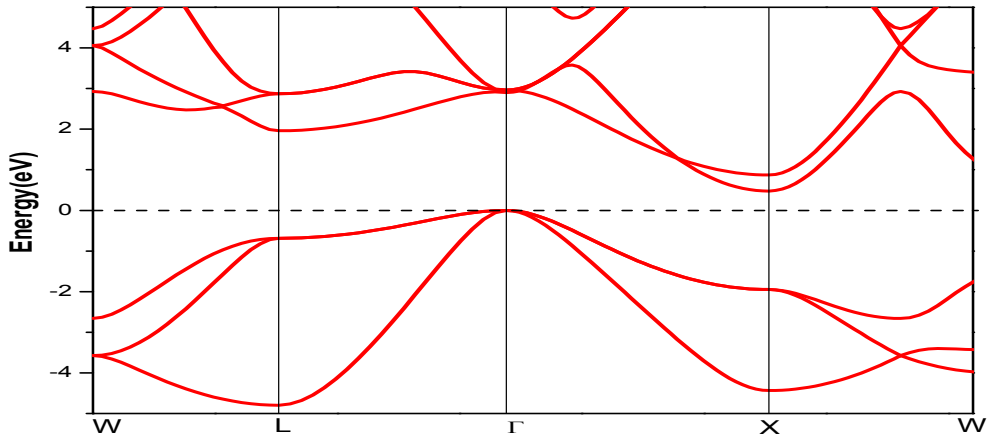

X=0 Mg_2Si

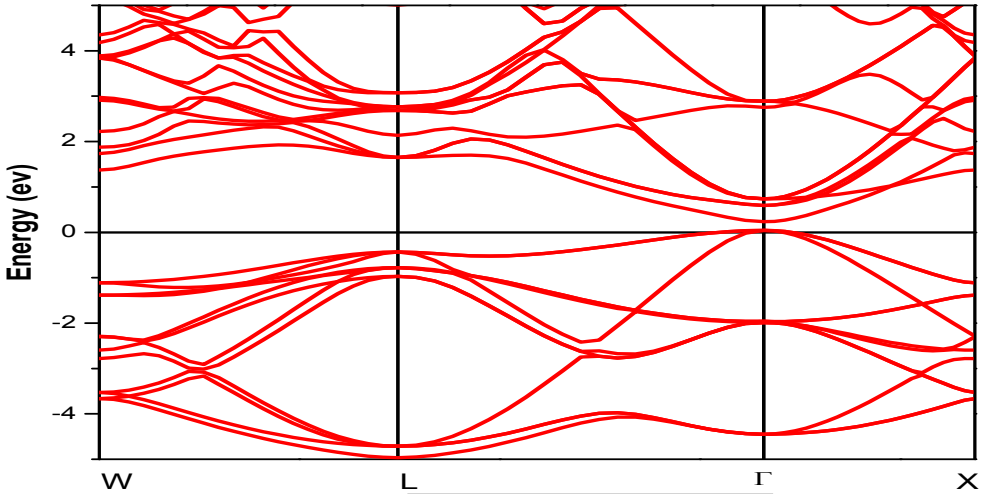

X=0,25 $Mg_2Si_{0.75}Sn_{0.25}$

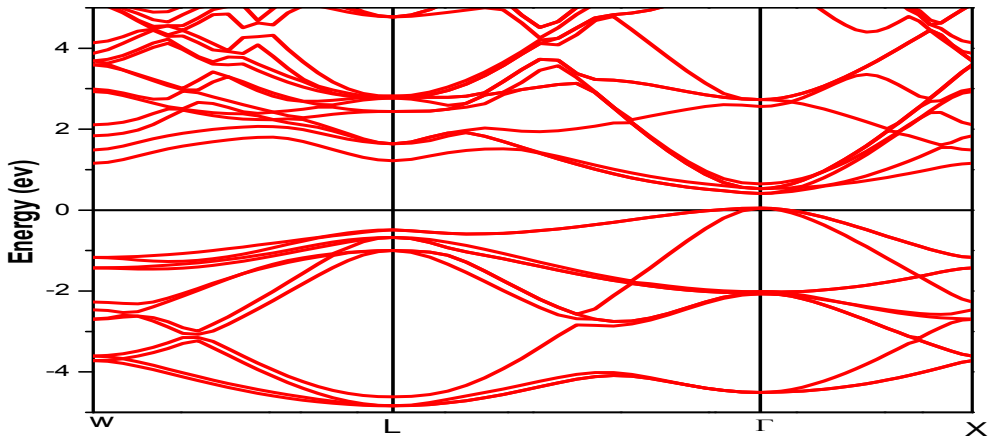

X=0,5 $Mg_2Si_{0.5}Sn_{0.5}$

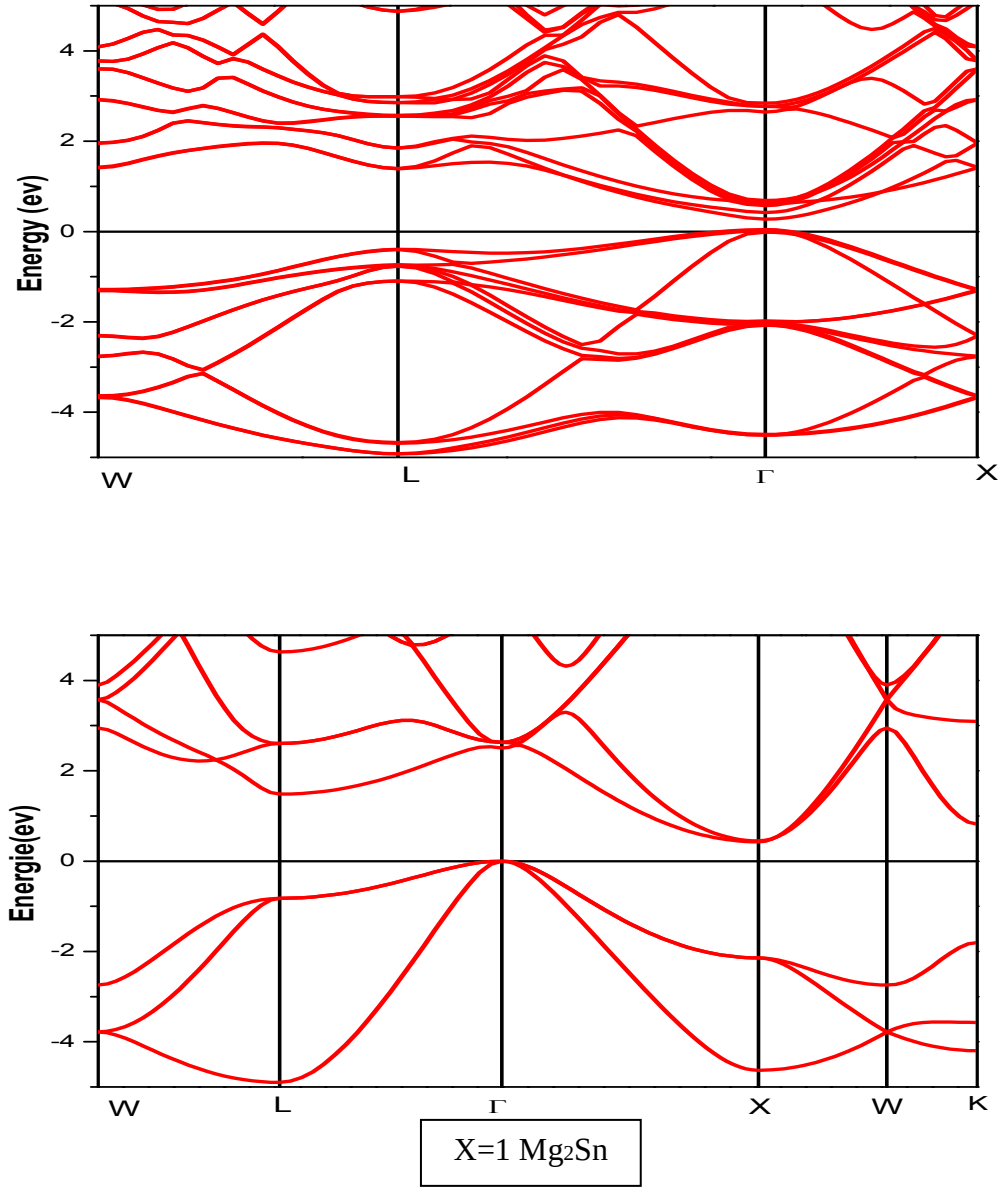

Figure III.4: structures of bands of $Mg_2Si_{1-x}Snx$ compounds (x = 0, 0.25, 0.5, 0.75, 1) ; Pressure P = 5Gpa

$Mg_2Si_{1-x}Sn_x$	Type of gap	mBJ, GGA(PBE)
x=0	Indirect	0,441
x=0,25	Direct	0,19
x=0,5	Direct	0,16
x=0,75	Direct	0,36
x=1	Indirect	0,36

Table III.4 : Gap values of our calculations (P = 5Gpa) and other work for Mg2Si1-xSnx at 0 GPa

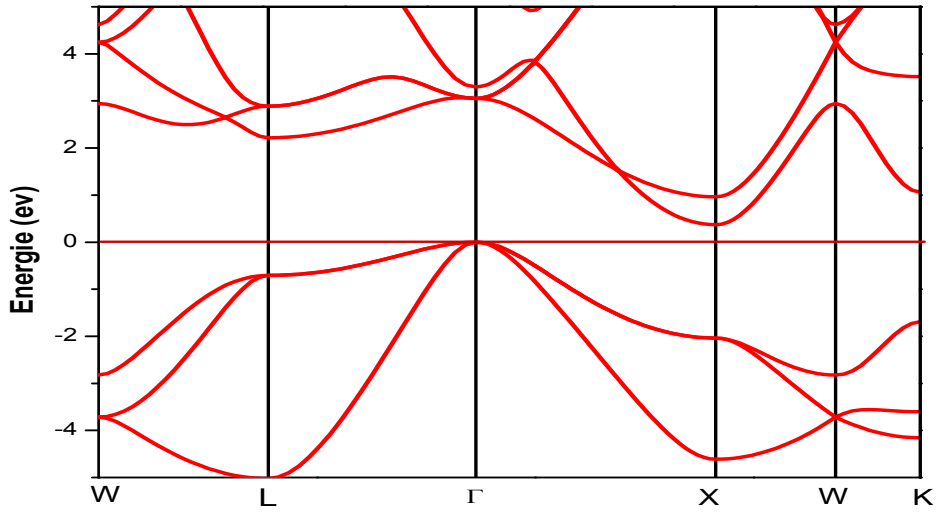

X=0 Mg_2Si

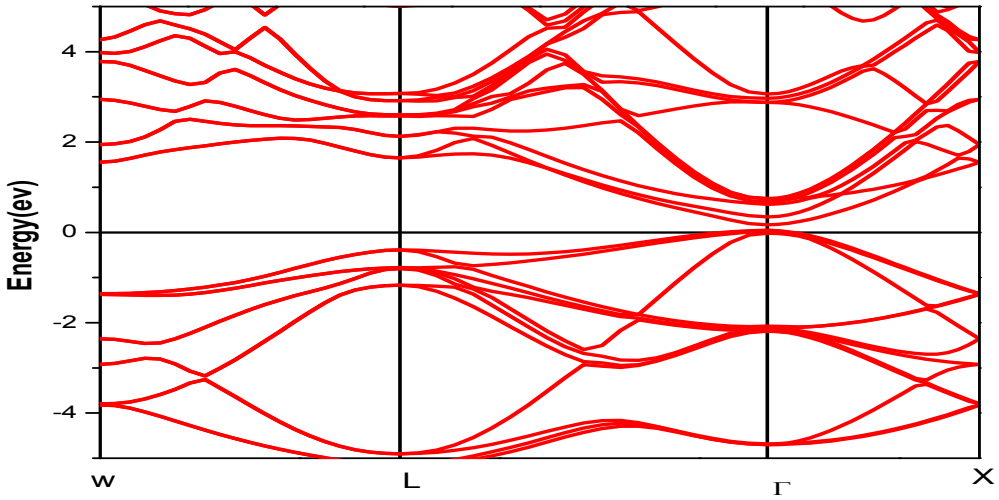

X=0,25 $Mg_2Si_{0.75}Sn_{0.25}$

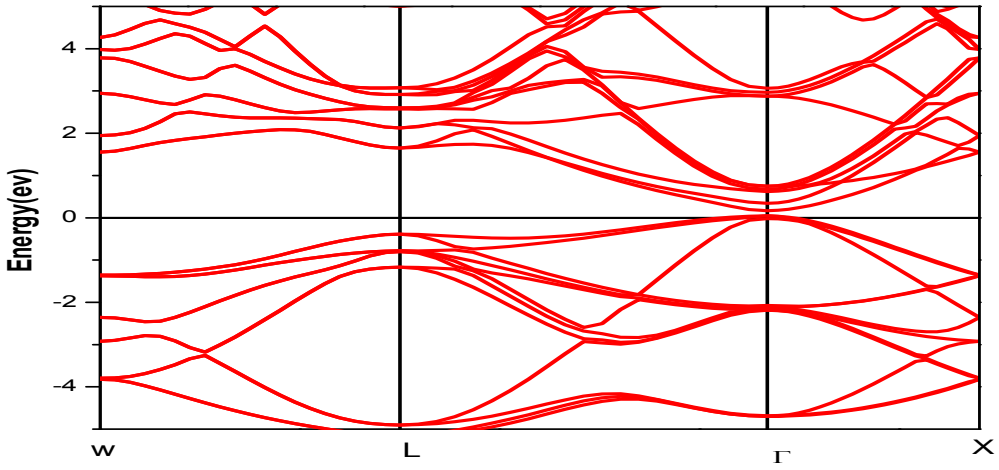

X=0,5 $Mg_2Si_{0.5}Sn_{0.5}$

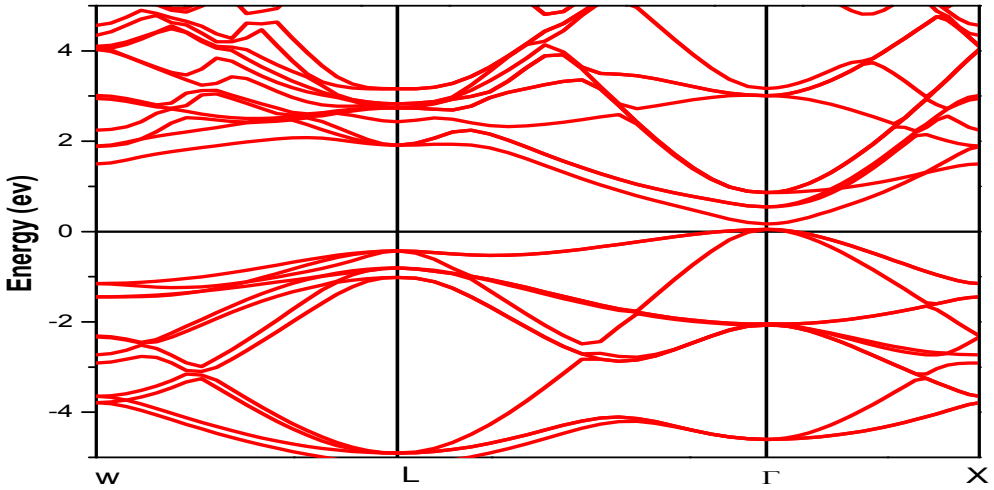

X=0,75 $Mg_2Si_{0.25}Sn_{0.75}$

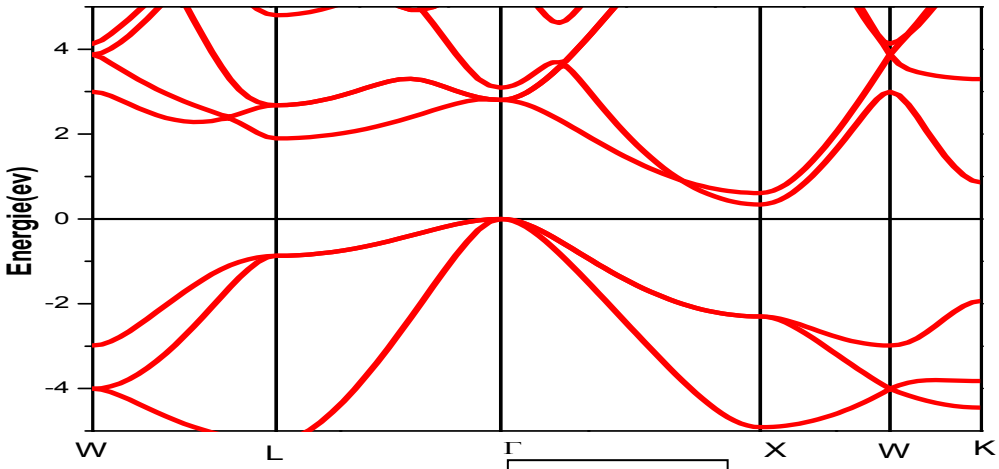

X=1 Mg_2Sn

Figure III.5: structures of bands of $Mg_2Si_{1-x}Snx$ compounds (x = 0, 0.25, 0.5, 0.75, 1) ; Pressure P =10Gpa

$Mg_2Si_{1-x}Sn_x$	Type de gap	mBJ, GGA(PBE)
x=0	Indirect	0,33
x=0,25	Direct	0,11
x=0,5	Direct	0,14
x=0,75	Direct	0,28
x=1	Indirect	0,31

Table III.5: gap values of our calculations (P = 10Gpa) and other work for Mg2Si1-xSnx at 0 GPa

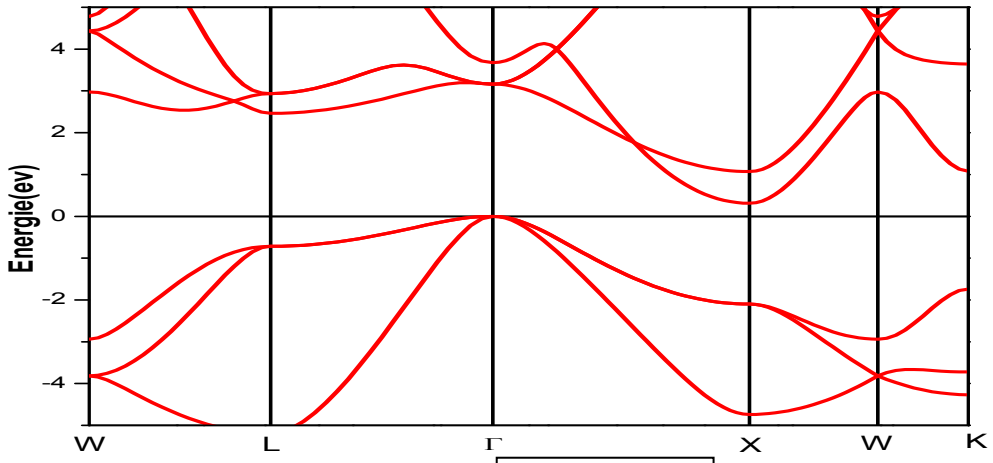

X=0 Mg_2Si

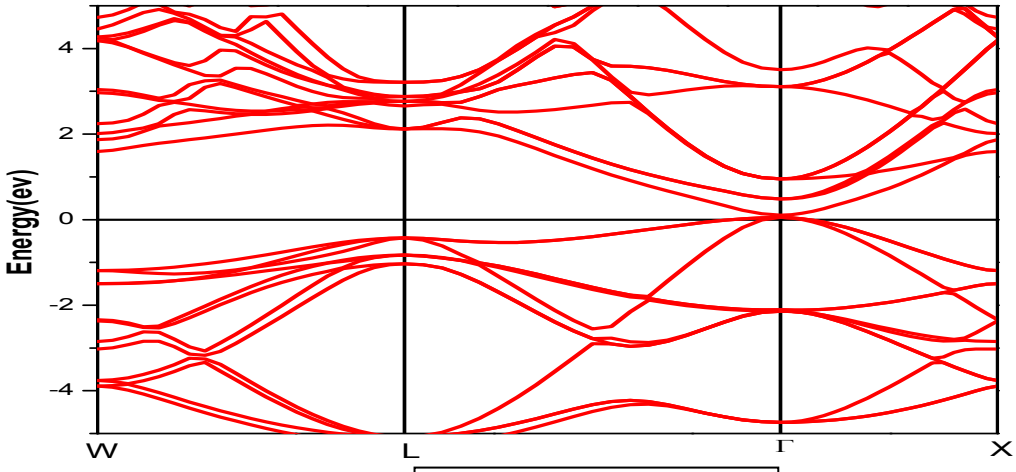

X=0,25 $Mg_2Si_{0.75}Sn_{0.25}$

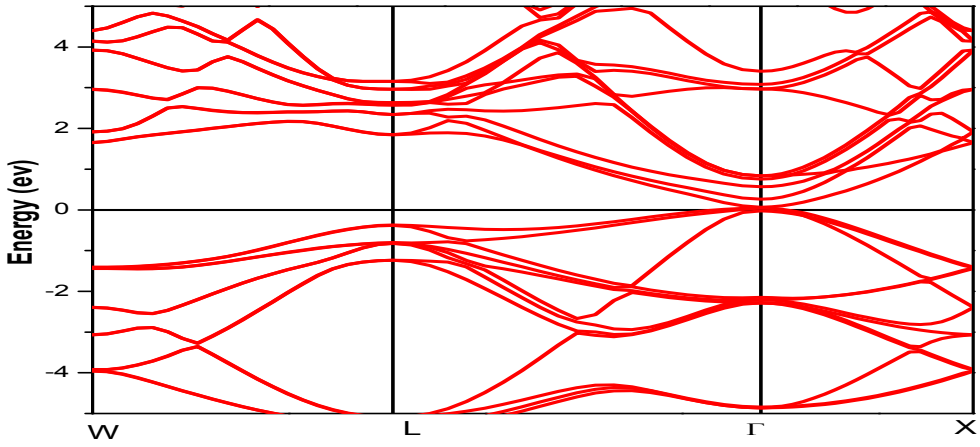

X=0,5 $Mg_2Si_{0.5}Sn_{0.5}$

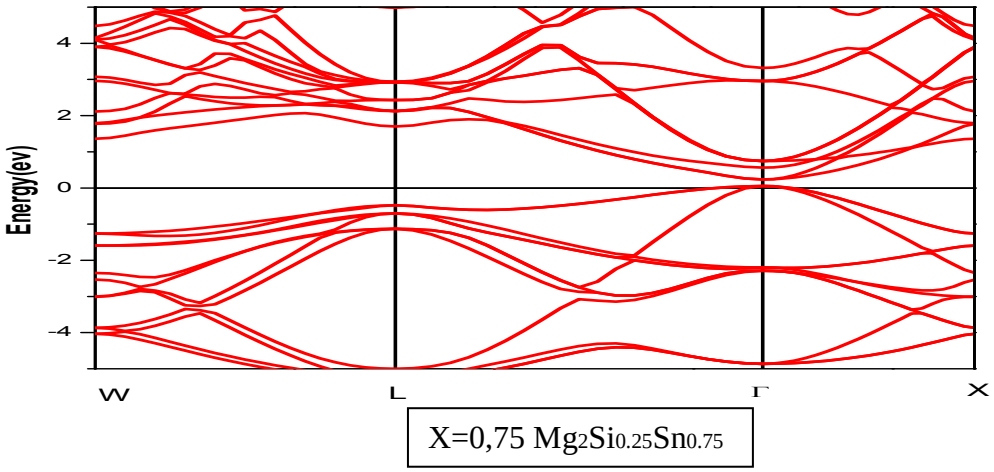

X=0,75 $Mg_2Si_{0.25}Sn_{0.75}$

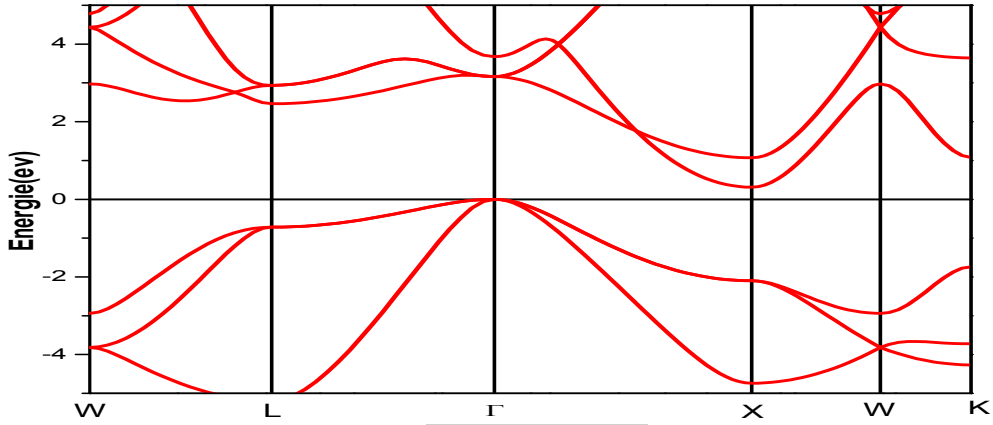

X=1 Mg_2Sn

Figure III.6: structures of bands of $Mg_2Si_{1-x}Sn_x$ compounds (x = 0, 0.25, 0.5, 0.75, 1) ; Pressure P =15Gpa

$Mg_2Si_{1-x}Sn_x$	Type de gap	mBJ, GGA(PBE)
x=0	Indirect	0,33
x=0,25	Direct	0,06
x=0,5	Direct	0,09
x=0,75	Direct	0,16
x=1	Indirect	0,25

Table III.6: gap values of our calculations (P = 15Gpa) and other work for Mg2Si1-xSnx at 0 GPa

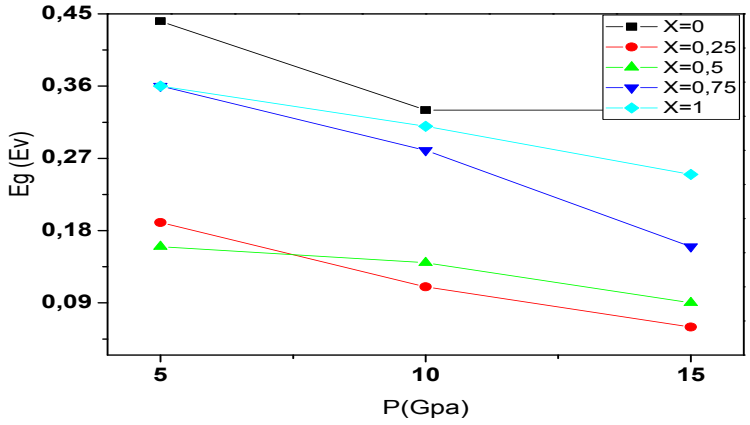

Figure III.6: Energy gap (Eg) a fct the presser (P)

III.4.2 Density of states (DOS):

To determine the nature of the electronic structure of bands, we calculated the total (DOS) and partial state (PDOS) densities of the compounds $Mg_2Si_{1-x}Snx$ (x = 0, 0.25, 0.5, 0.75, 1) at pressure (P = 5 Gpa, 10Gpa and 15Gpa).

For(x=0; 1) :

The valence states are divided into two parts: a part situated in the domain [-9.15, -7.1] eV, which is formed by the states s of Si (Sn) and the two states of Mg, s and p. The second part is in the domain [-4.9, -0.1], it is dominated by the states p of Si (Sn) and the states s and p of Mg, with weak contributions of the state's s of Si (Sn) and of from Sn.

The effect of presser in the stat **S** of **Mg** in BC(diminishing)

For (x=0,25; 0,75) :

The valence states of $Mg_2Si_{0.75}Sn_{0.25}$ and $Mg_2Si_{0.25}Sn_{0.75}$ are characterized by two intervals, the first energy range [-9.3, -7.1] eV, is dominated by a participation of the state s of Si and Sn and the state s and p of Mg. The energy interval [-4.98, -0.1] eV which expresses the states of the second part, is dominated by the contribution of the state's s and p of Mg, p of Si and s of Sn, with a very small contribution of the state's s of Si and Sn.

The effect of presser in the stat **P** of **Sn** (diminishing) (X=0,25)

The effect of presser in the stat **S**, **P** of **Mg** (diminishing) for (X=0,75)

For (x=0,5)

In the case of $Mg_2Si0.5Sn0.5$, the valence states are given by two parts: the first is defined in [-9.21, -6.94] eV by the contribution of the state's s of Si and Sn , and states s and p of Mg. The second part is presented in the interval [-4.69, -0.46] eV, it is dominated by the states s, p of Si and Sn and the states s and p of Mg.

For the conduction region, for the compound Mg 2 Si (Sn), a dominance of the state's s and p of Mg is observed, as well as the p states of Si (Sn) and the states d for the compound Mg_2Sn; likewise for the solid solution $Mg_2Si_{1-x}Snx$ (X = 0.25, 0.5, 0.75), can conclude then that the valence region is dominated by the states s and p of the Mg and p of the Si and Sn atoms for our $Mg_2Si_{1-x}Snx$ (x = 0, 0.25, 0.5, 0.75, 1). as shown in **Figure III.(7,8,9).**

The effect of presser in the stat **P** of **Sn** (diminishing)

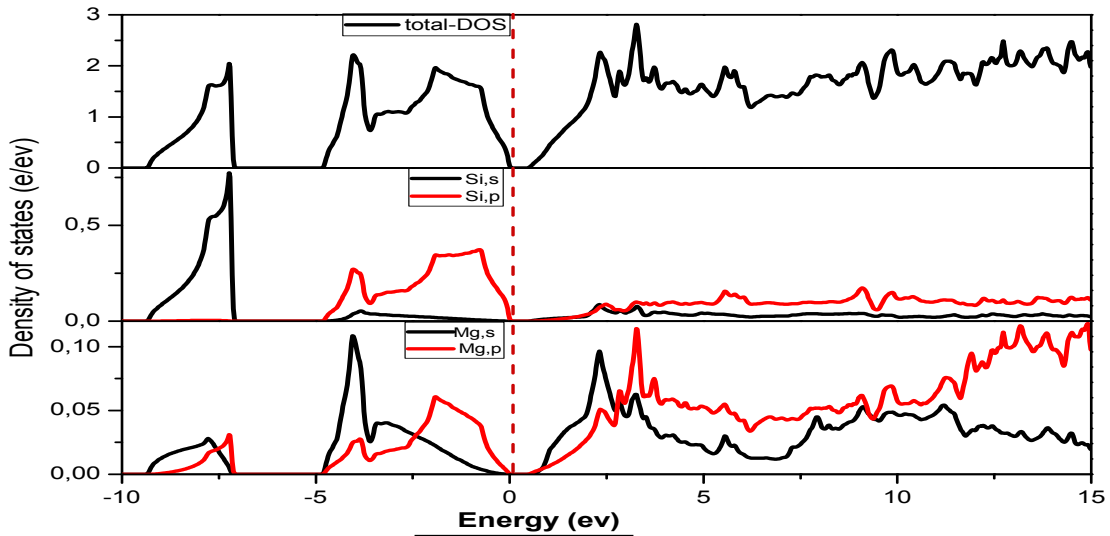

X=0 Mg_2Si

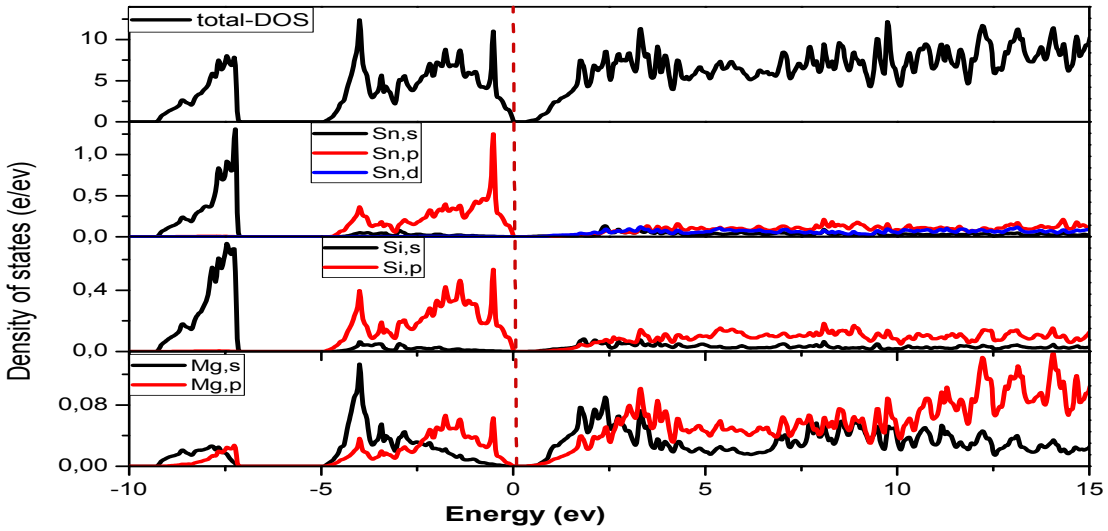

X=0,25 $Mg_2Si_{0.75}Sn_{0.25}$

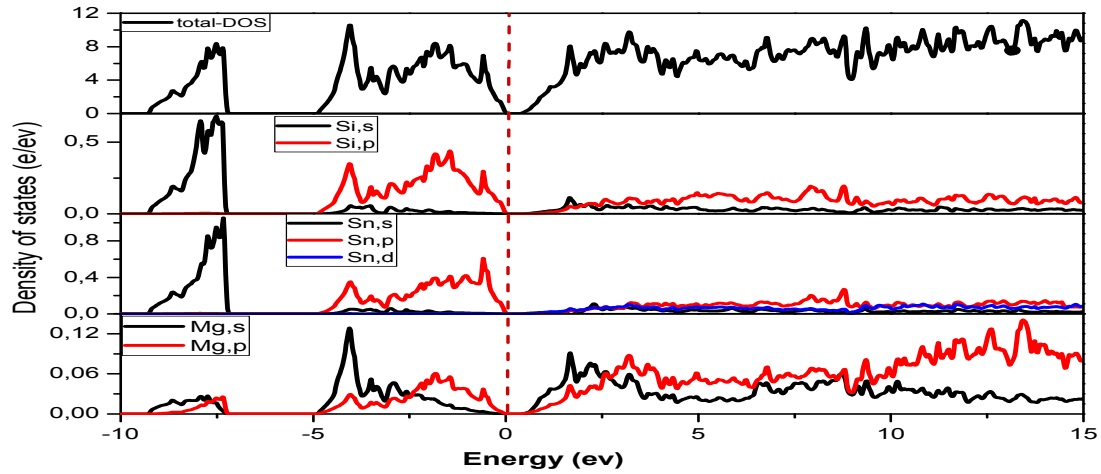

X=0,5 $Mg_2Si_{0.5}Sn_{0.5}$

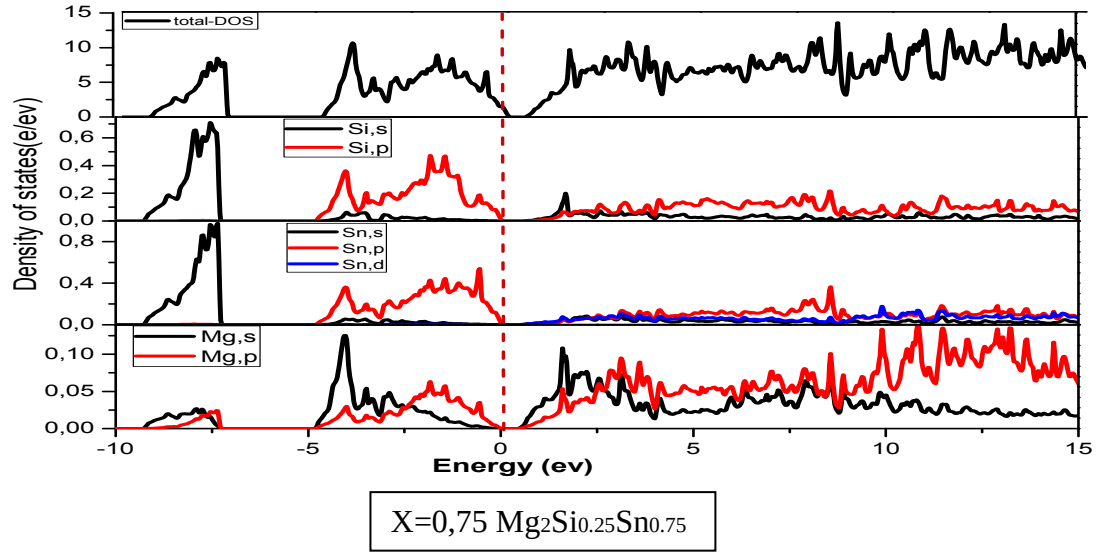

X=0,75 $Mg_2Si_{0.25}Sn_{0.75}$

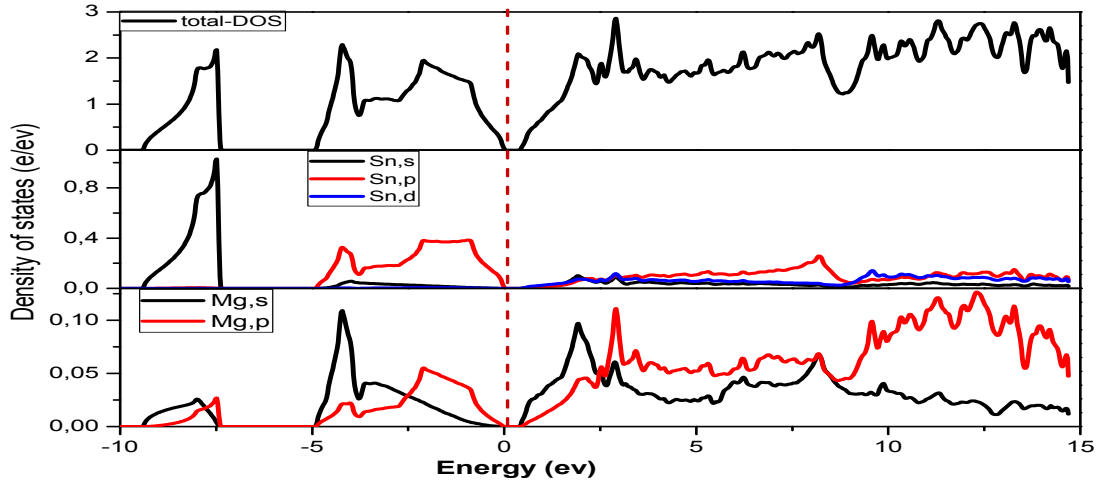

X=1 Mg_2Sn

Figure III.7: The total and partial states density of the compounds $Mg_2Si_{1-x}Snx$ (x=0, 0.25, 0.5, 0.75, 1) ; P=5Gpa

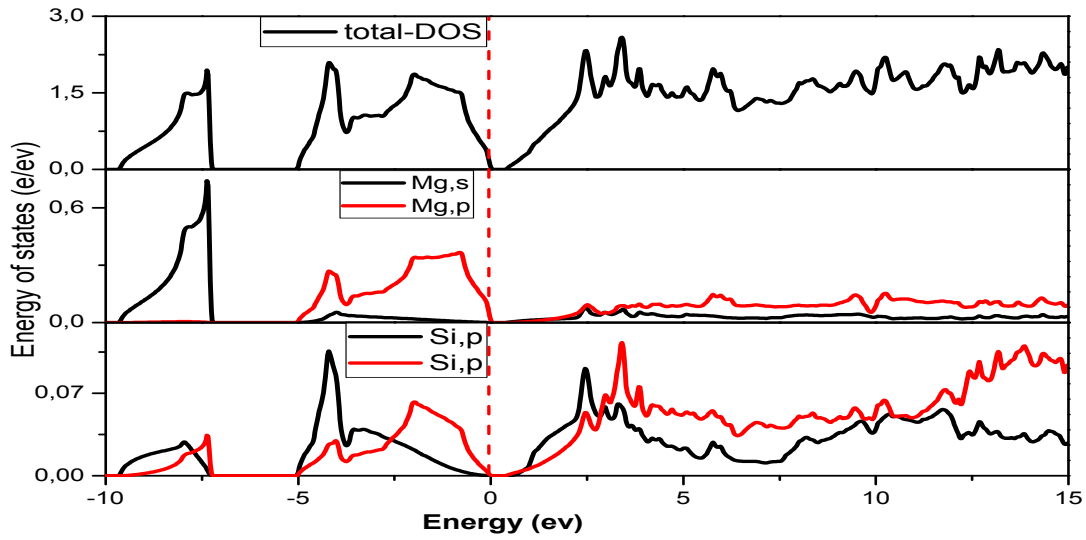

X=0 Mg_2Si

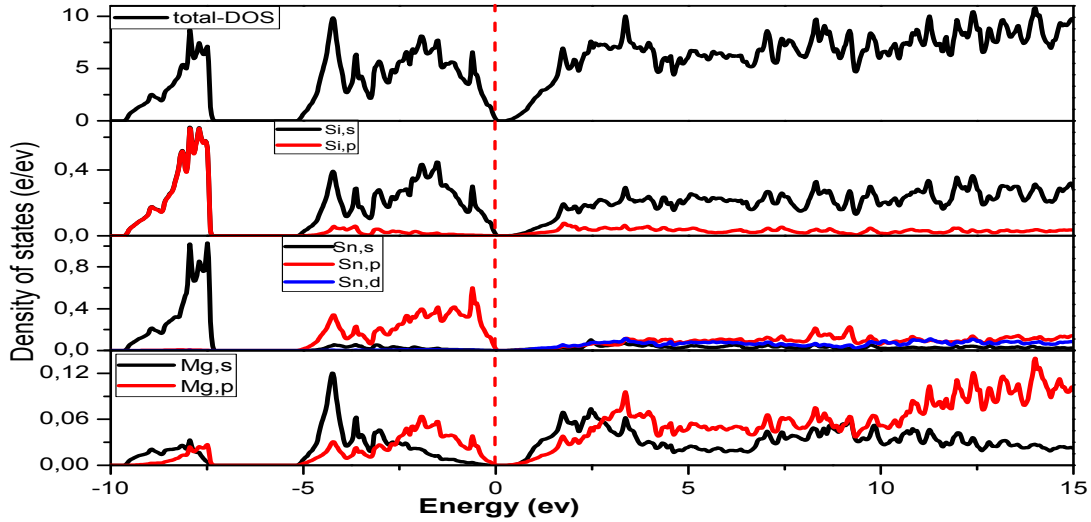

X=0,25 $Mg_2Si_{0.75}Sn_{0.25}$

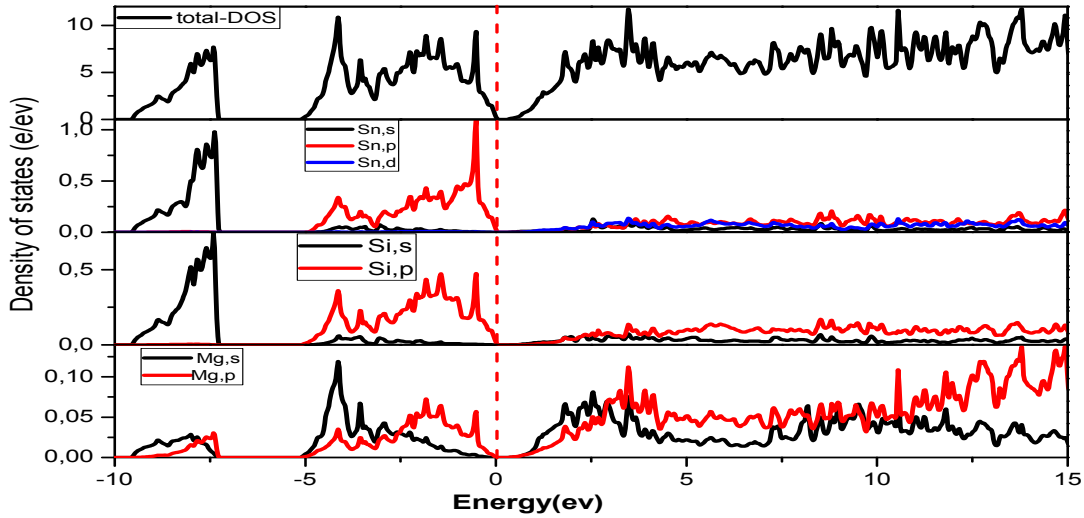

X=0,5 $Mg_2Si_{0.5}Sn_{0.5}$

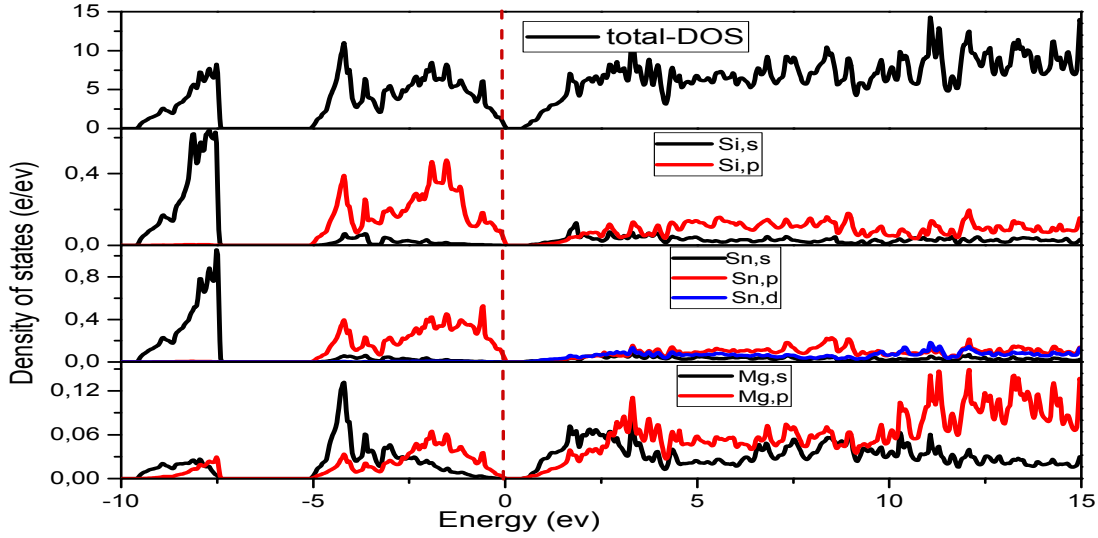

X=0,75 $Mg_2Si_{0.25}Sn_{0.75}$

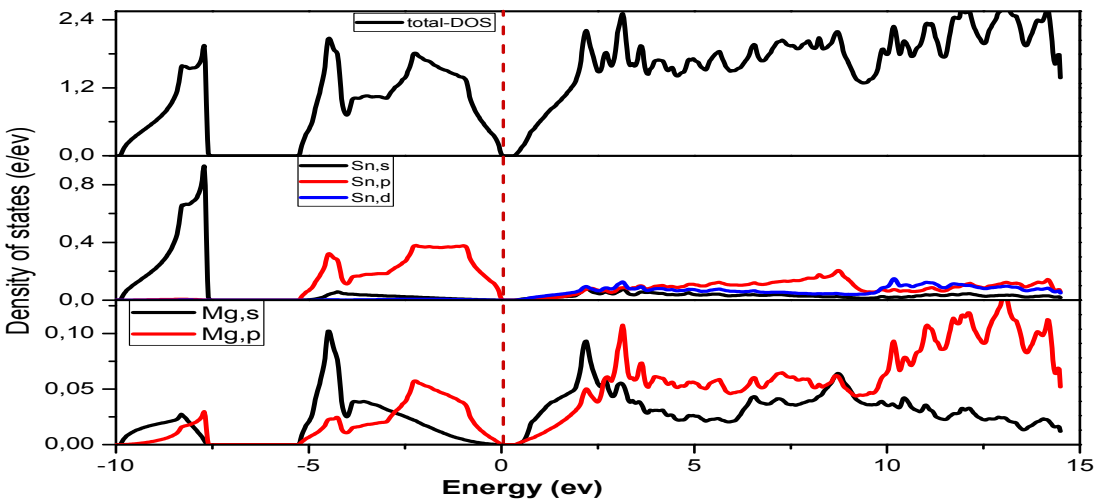

X=1 Mg_2Sn

Figure III.8: The total and partial states density of the compounds $Mg_2Si_{1-x}Snx$ (x=0, 0.25, 0.5, 0.75, 1) ; P=10Gpa

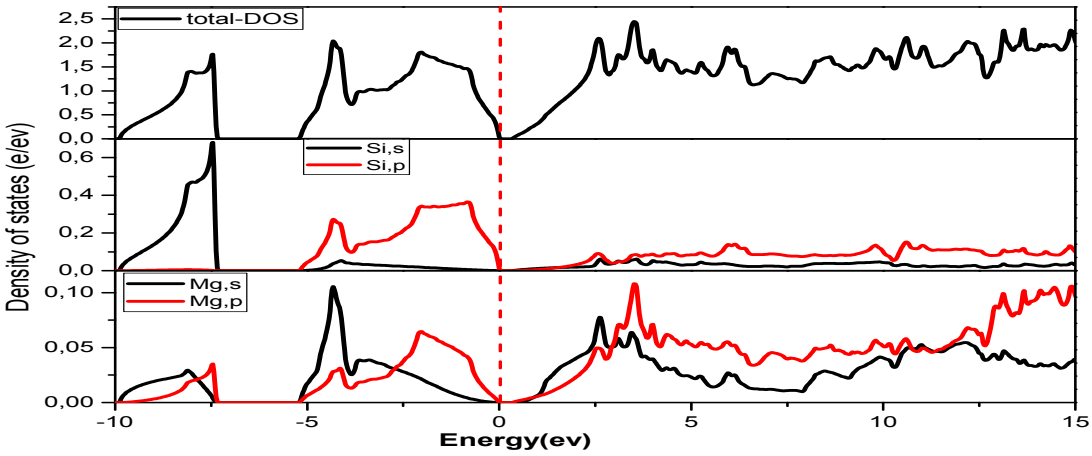

X=0 Mg_2Si

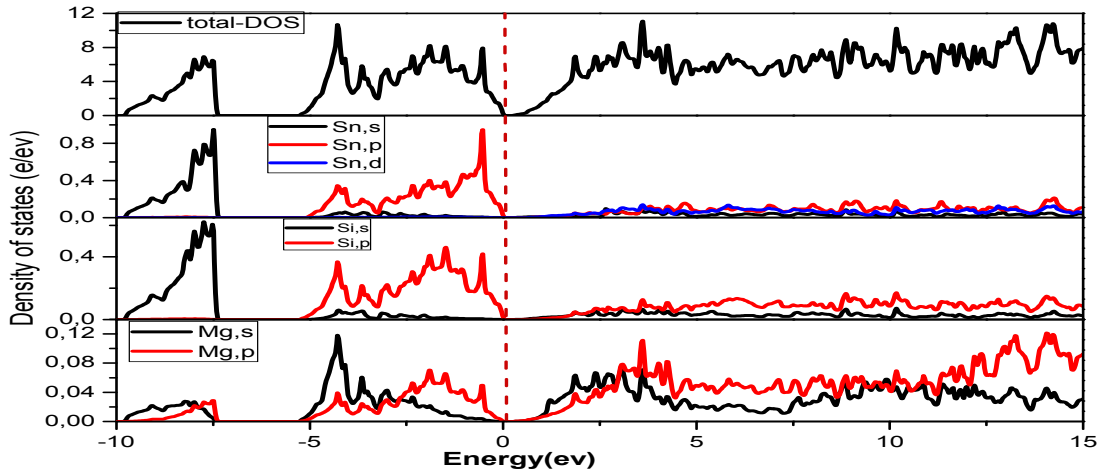

X=0,25 $Mg_2Si_{0.75}Sn_{0.25}$

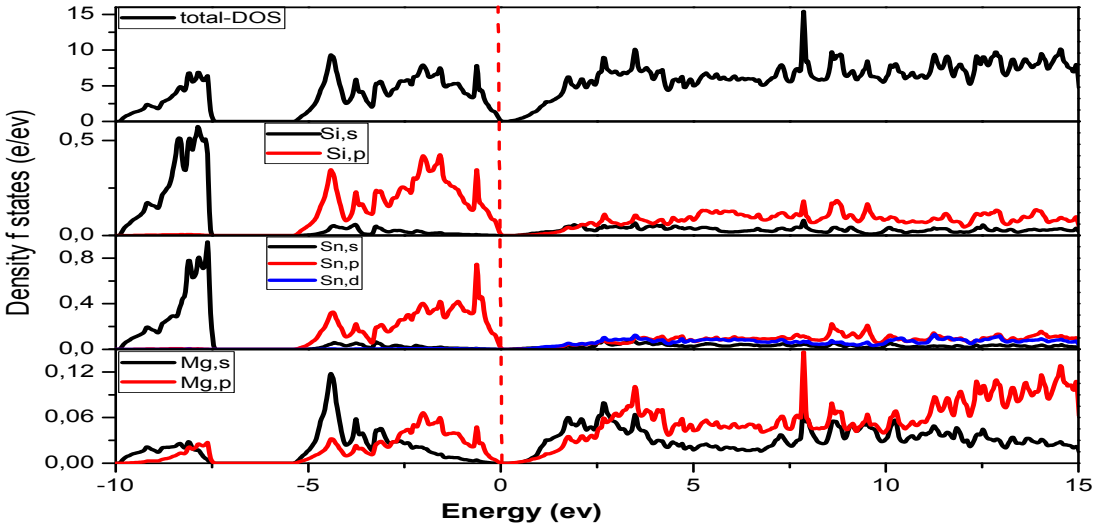

X=0,5 $Mg_2Si_{0.5}Sn_{0.5}$

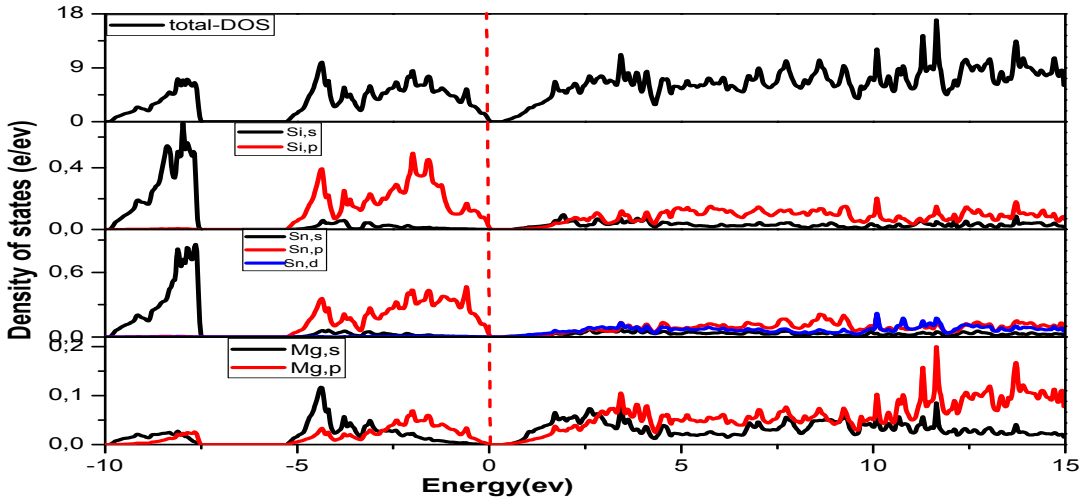

X=0,75 $Mg_2Si_{0.25}Sn_{0.75}$

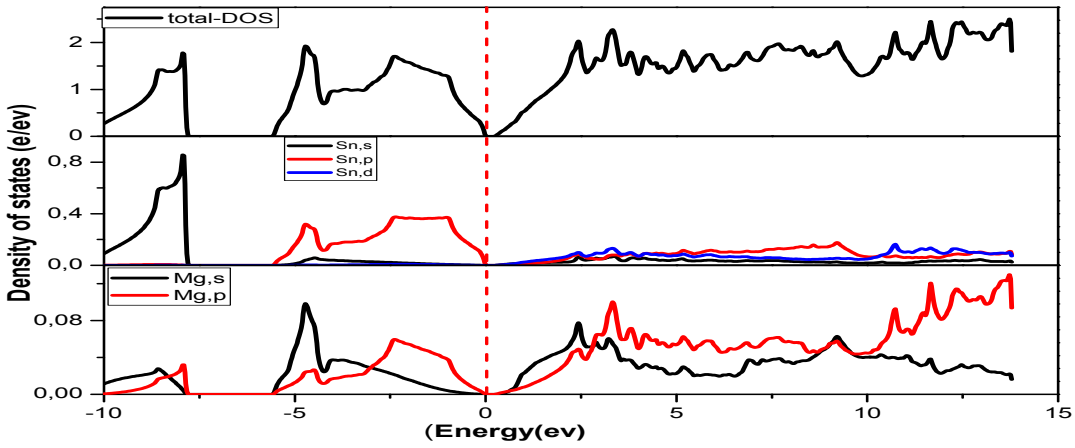

X=1 Mg_2Sn

Figure III.9: The total and partial states density of the compounds $Mg_2Si_{1-x}Snx$ (x=0, 0.25, 0.5, 0.75,1) ; P=15Gpa

III.5 Transport properties:

The calculation of thermoelectric transport properties such as electrical conductivity (σ), Seebeck coefficient (S), power factor ($S^2.\sigma$) and electronic thermal conductivity (λ) was limited to $Mg_2Si_{1-x}Snx$ compounds. Default time and tools code has been used to the BoltzTraP, by solving the Boltzmann linear equation in the approximation of the relaxation time τ, these properties are related to the energy band gap values obtained through the DFT calculations.

On the basis of the calculated energy band structure and the density of the states, the electrical conductivity is calculated with the constant diffusion time relaxation approximation (τ), expressed as the ratio σ / τ.

III.5.1 Electrical conductivity:

The electrical conductivity of $Mg_2Si_{1-x}Snx$ (x = 0, 0.25, 0.5, 0.75, 1) at pressure (P = 5Gpa ; 10Gpa; 15Gpa) and doping P-type (n = 10^{19}; 10^{20}, n = 10^{21}) as a function of temperatures for a fixed chemical potential , the electrical conductivity increases monotonically with the increase of temperatures of 300 K ° which confirm the high temperature domain for doping (n = 10^{19}) and the increase of temperatures of 700 K ° which confirm the high temperature domain for doping (n = 10^{20}), and for (n = 10^{21}) increases linearly with increasing temperatures .

III.5.2 The Seebeck coefficient:

The Seebeck coefficient (S) is related to the electronic structure of materials, the results calculated as a function of temperatures for a fixed chemical potential are presented in Figure , we can observe for pressure (P = 5Gpa ; 10Gpa ; 15Gpa) and doping P-type (n = 10^{19}, n = 10^{20}, n =10^{21}) the positive sign of S indicated. . One can also observe a very strong increase of the value of S with the increase of the temperature, to confirm the dependence of S on the changes of temperature, the maximum value of the Seebeck coefficient for and doping (n = 10^{19}) between 300-600 K °, which again confirms the high temperature range for this system, and in the doping (n = 10^{20}; n = 10^{21}) value of S is increased by the temperature.

III.5.3 Thermal conductivity:

The thermal conductivity of the λ_{ph} network(Lattice) and the electronic thermal conductivity contribute to the total thermal conductivity which consists of electronic contributions and phonon (phonons across the lattice), BoltzTraP calculates the electronic part taking into account the relaxation time constant (τ), generally in the theoretical model, we ignore the thermal conductivity of the λ_{ph} network and we are interested in the electronic part of the thermal conductivity λ_{ele} because it is not easy to predict λ_{ph} from ab initio calculations or molecular simulations, the electronic thermal conductivity λ_{ele} for the compounds $Mg_2Si_{1-x}Snx$ (x = 0, 0.25, 0.5, 0.75; 1) at the pressure (P = 5; 10; 15Gpa) and doping P-type (n = 10^{19}; n = 10^{20}, n

= 10^{21}) as a function of τ for a fixed chemical potential presented in Figure , shows an exponential increase in the thermal conductivity λ_{ele} of Mg_2Si-Mg_2Sn, when the temperature increases from 100 to 1000 K °, and this is due to the heat that is transported from the warm side to the cold side in a very fast manner. as shown in **Figure III.(10,11,12).**

III.5.4 The power factor:

The power factor ($S^2.\sigma$ / τ) shown in Figure can be calculated from the Seebeck S coefficient and electrical conductivity. The power factor is as numerator in the merit relation ($ZT = S^2. \sigma / \lambda$), therefore, this is a very important amount for calculating the transport properties of materials, we can see that the power factor for $Mg_2Si_{1-x}Snx$ compounds (x = 0; 0.25; 0.5; 0.75 ; 1) at the pressure (P = 5; 10; 15Gpa)

- X=0 Effect pressers in the doping P-type n = 10^{20} (increases with increasing temperature to the range of 300-800 K)
- X=0,25 Effect pressers in the doping P-type n = 10^{19} and n=10^{20} (increases with increasing temperature to the range of 300-800 K)
- X=0,5 Effect pressers in the doping P-type n = 10^{19} and n=10^{20} (increases with increasing temperature to the range of 300-800 K)
- X=0,75 Effect pressers in the doping P-type n = 10^{21} (increases with increasing temperature to the range of 300-800 K)
- X=1 Effect pressers in the doping P-type n = 10^{20} (increases with increasing temperature to the range of 300-800 K), as shown in **Figure III.(13).**

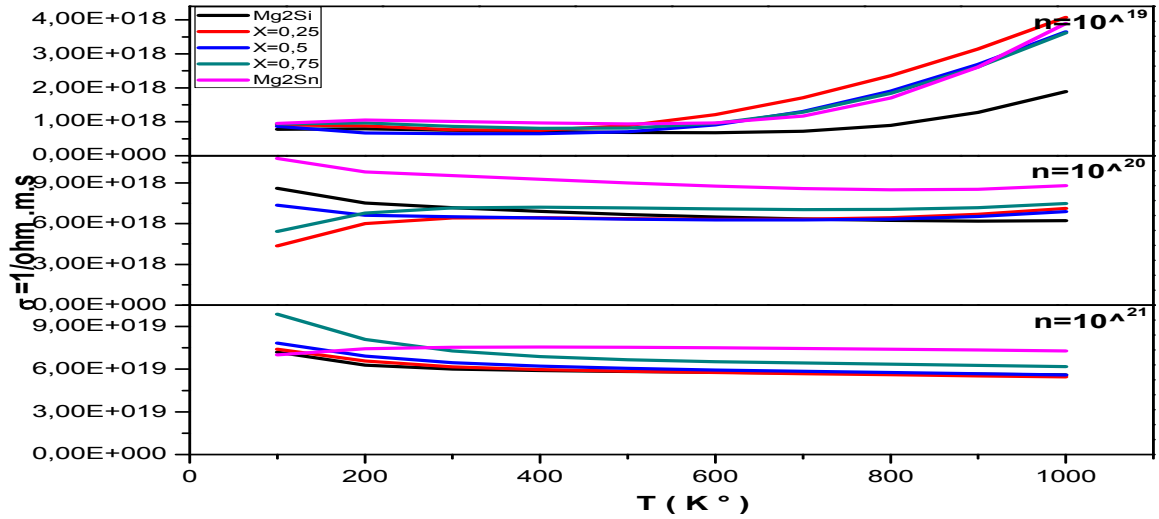

Electrical conductivity; P=5Gpa

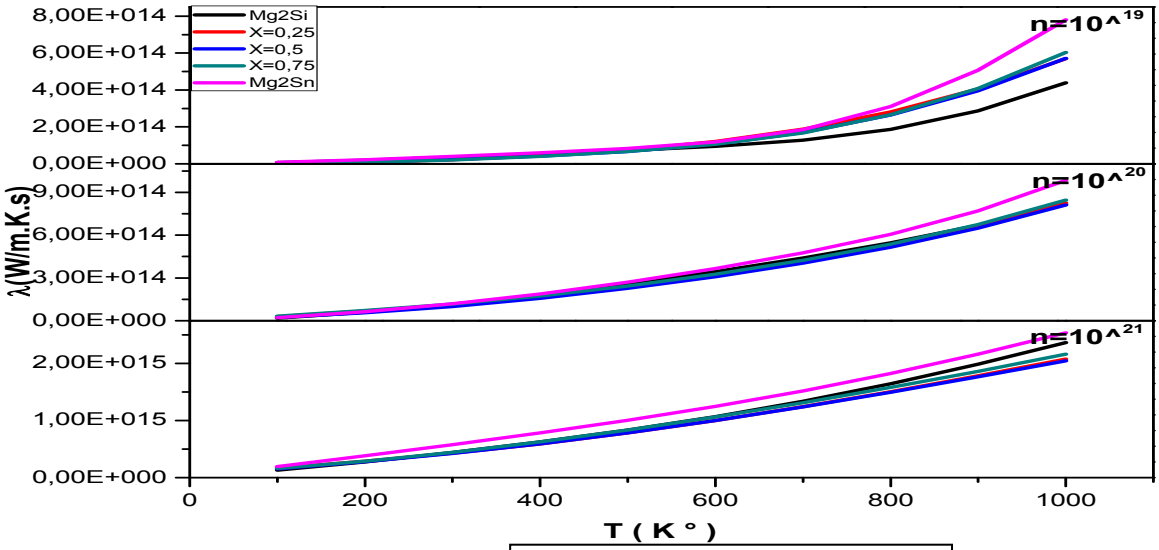

Thermal conductivity; P=5Gpa

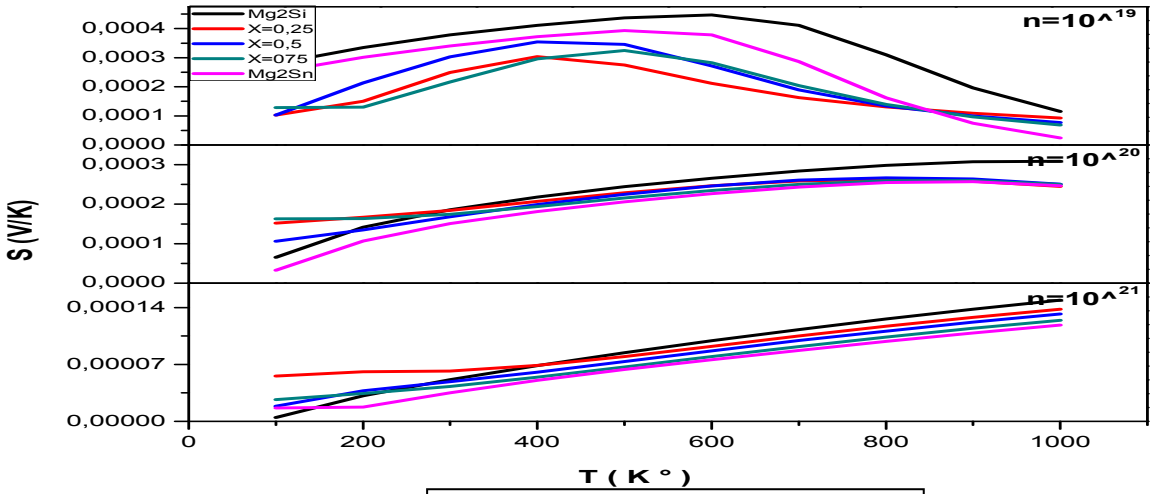

The Seebeck coefficient; P=5Gpa

Figure III.10: Electrical conductivity; Thermal conductivity and The Seebeck coefficient of P=5Gpa

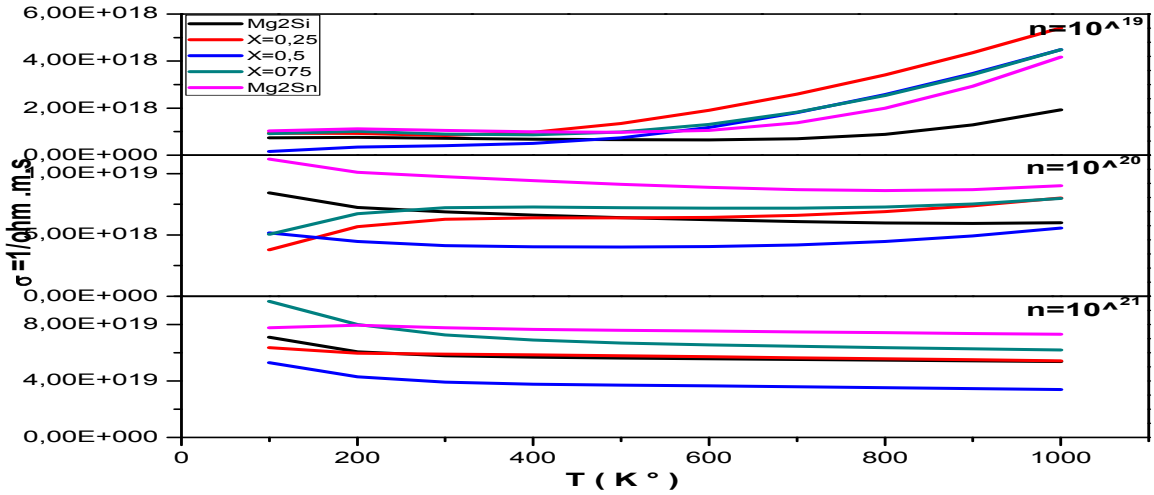

Electrical conductivity; P=10Gpa

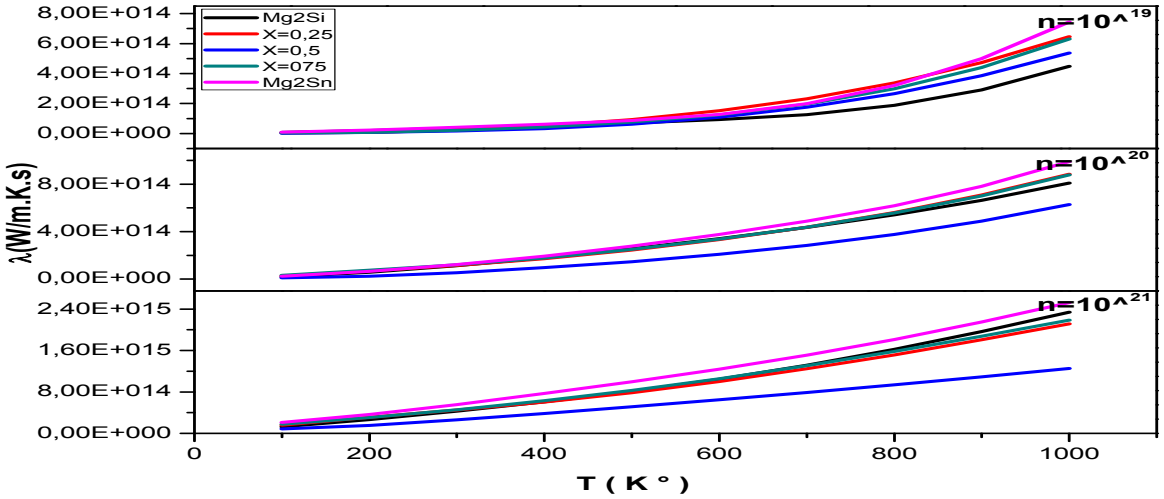

Thermal conductivity; P=10Gpa

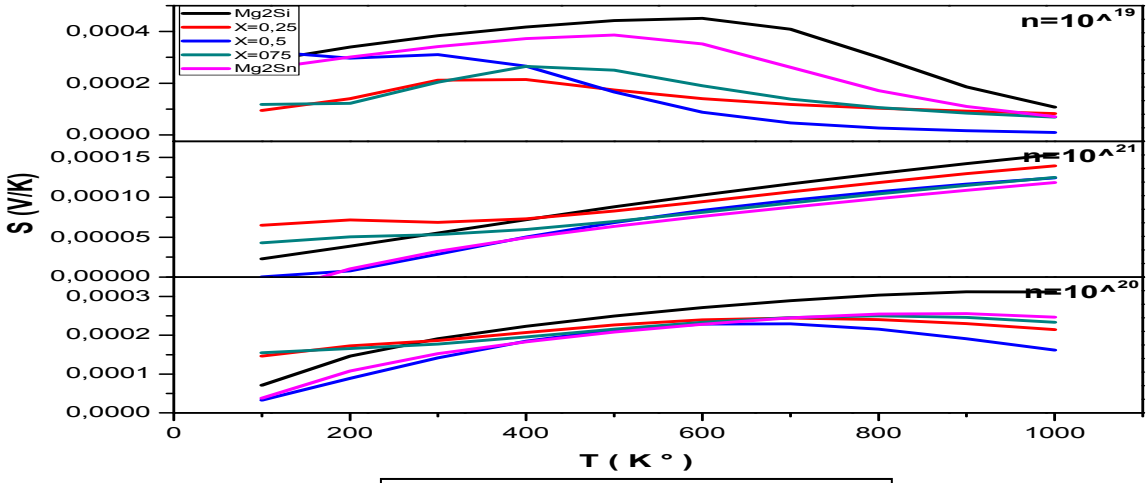

The Seebeck coefficient; P=10Gpa

Figure III.11: Electrical conductivity; Thermal conductivity and The Seebeck coefficient of P=10Gpa

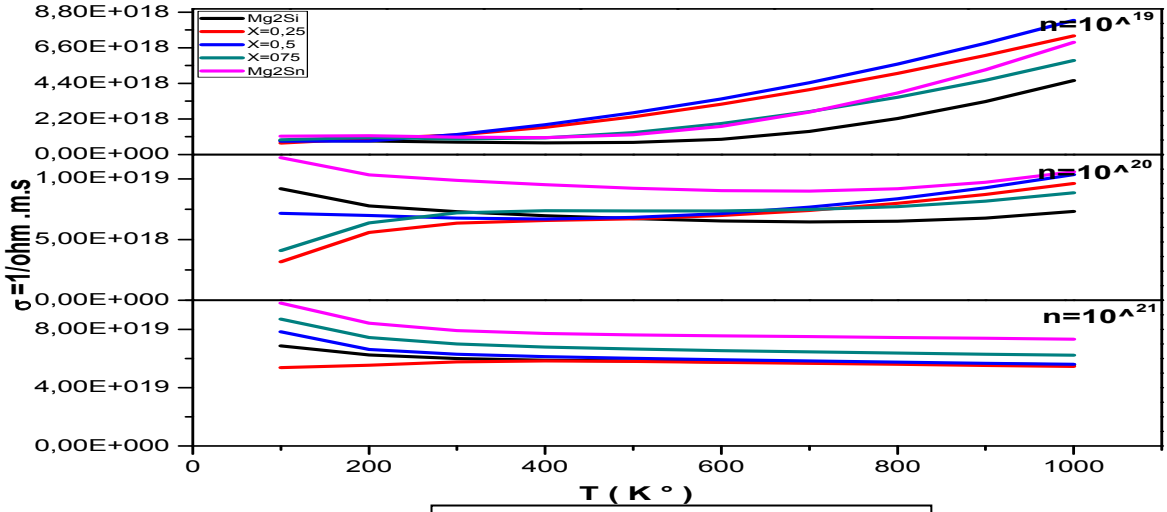

Electrical conductivity; P=15Gpa

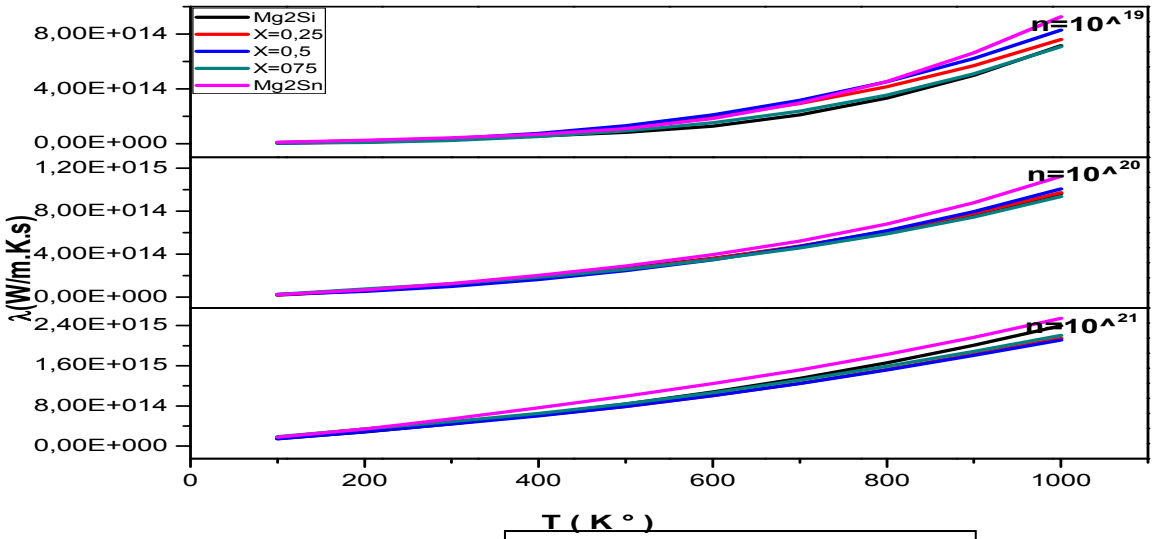

Thermal conductivity; P=15Gpa

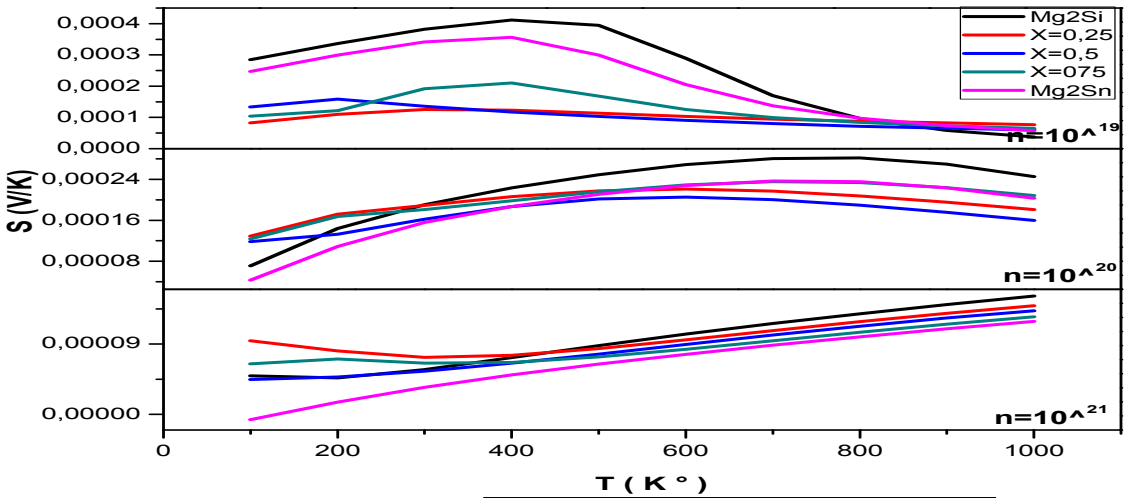

The Seebeck coefficient; P=15Gpa

Figure III.12: Electrical conductivity; Thermal conductivity and The Seebeck coefficient of P=15Gp

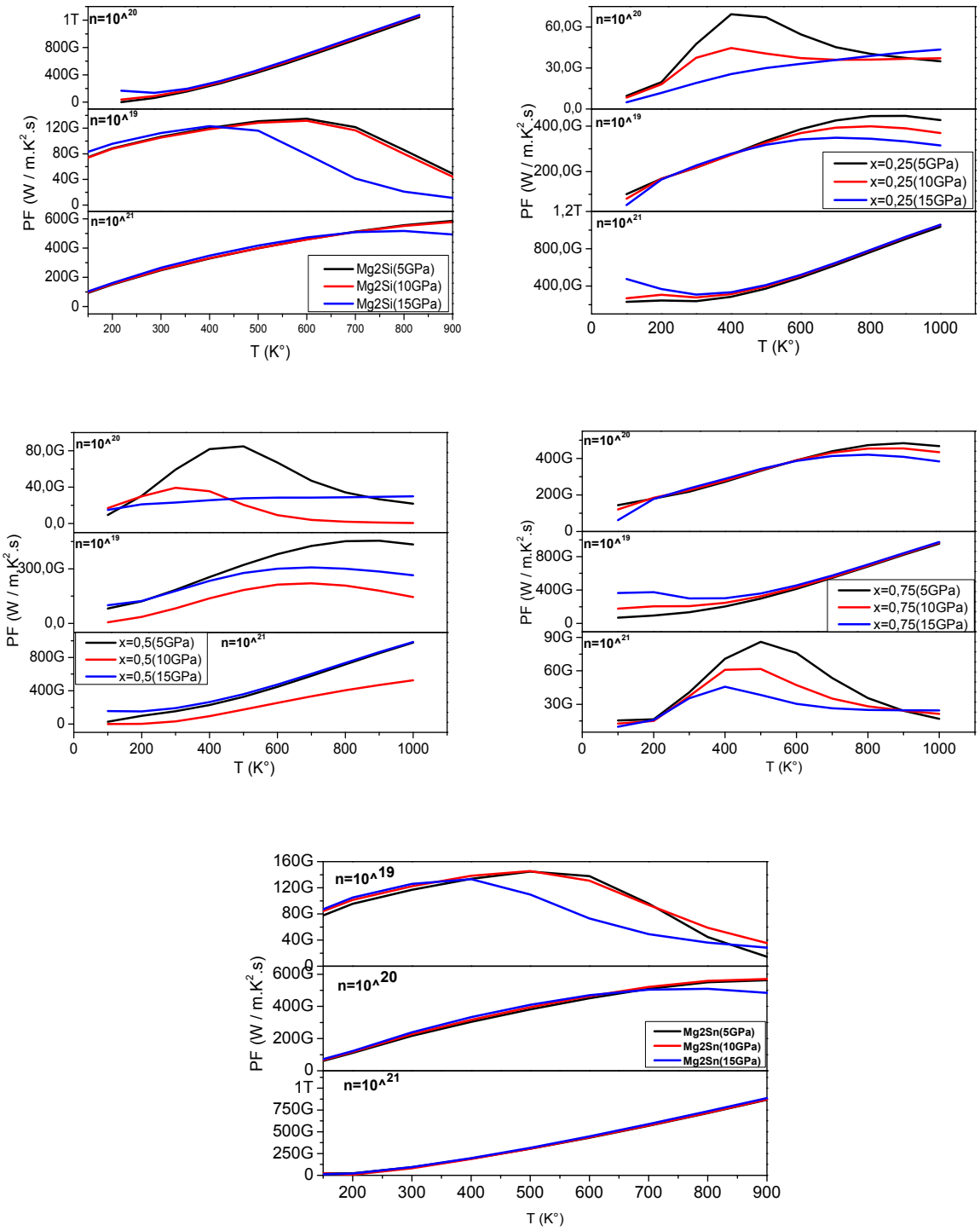

Figure III.13: The power factor of (P=5Gpa; P=10Gpa and 15Gpa) and P-type (n = 10^{19}; 10^{20}, n = 10^{21})

III.6Conclusion:

In this work, we carried out a theoretical study using the augmented and linearized flat wave method (FP-LAPW), based on the density functional theory (DFT) implemented in the WIEN2K code, to determine the structural and electronic properties of the compounds Mg2Si1-xSnx (x = 0.0.25, 0.5, 0.75, 1) at pressure (P = 5Gpa, 10Gap, 15Gpa), thus, the calculation of transport properties by semi-classical BoltzTraP methods. Exchange potential and correlation (XC) is processed by the local density approximation (LDA), the generalized gradient approximation (GGA) and the modified Beck Jonhson approximation (mBJ).

In the present case, the energy gap **Eg** a decreases with increasing pressure. and the effect in **DOS** of presser in the stat, stat a decreases with increasing pressure. and for the power factor **PF** increases with increasing temperature to the range of 300-800 K.

Bibliography

CHAPTER 1

[1] B. Roux, *La Thermoélectricité Etude bibliographique*. 2008.

[2] B. ZOUAK, « Etude de l'évolution des caractéristiques des matériaux thermoélectriques des anciennes et nouvelles générations et applications photovoltaïque-thermoélectricité . Devant le jury d'examen », 2012.

[3] M. Rowe, Éd., *Thermoelectrics handbook: macro to nano*. Boca Raton: CRC/Taylor & Francis, 2006.

[4] G. Nolas, J. Sharp, et J. Goldsmid, *Thermoelectrics: basic principles and new materials developments*. Berlin; New York: Springer, 2010.

[5] G. Rico, « THERMOELECTRIC PROPERTY STUDY OF N-TYPE PBTE », 2014.

[6] M. Kishi , « Micro thermoelectric modules and their application to wristwatchesas an energy source », in 18th International Conference on Thermoelectrics, 1999, p. 301-307.

[7] L. Bell, « Cooling, heating, generating power, and recovering waste heat with thermoelectric systems », Sciencce, vol. 321, no. 5895, p. 1457-1461, 2008.

[8] F.Jean , « Vehicular Thermoelectric Applications », the 6th European Conference on Thermoelectrics, paris-2008.

[10] Z.Veljko. Alex C. Hewson, « Properties and Applications of Thermoelectric Materials», P. 345 September 2008.

[11] H. Jean. Goldsmid, Introduction to Thermoelectricity. Springer, 2009.

[12] Q. Huy Le, « Matériaux thermoélectriques du type Mg2Si–Mg2Sn élaborés en couches minces par co-pulvérisation assistée par plasma », Grenoble, 2011.

[13] J. R. Sootsman, D. Chung, et M.Kanatzidis, « New and Old Concepts in Thermoelectric Materials », *Angew. Chem. Int. Ed.*, vol. 48, n° 46, p. 8616‑8639, nov. 2009.

[14] P.X.Zhang « New thermoelectric materials and new applications». Institute of advanced materials for photo electronics, volume 27n°1, 2004.

[15] Z. et al V. K., « Highly effective Mg2Si1-xSnxthermoelectrics », *Phys. Rev. B*, vol. 74, 2006.

[16] N. et al E. N, « Thermoelectric properties of solid solutions Mg2Si-Mg2Sn », vol. 3, p. 2648‑2651, 1962.

[17] « Thermoelectric elements based on compounds of silicon and transition metals », *Tech. Phys. Lett.*, vol. 23, p. 602‑603, 1997.

[18] G. H. Grosch et K.-J. Range, « Studies on AB2-type intermetallic compounds, I. Mg2Ge and Mg2Sn: single-crystal structure refinement and ab initio calculations », *J. Alloys Compd.*, vol. 235, n° 2, p. 250‑255, mars 1996.

[19] V. Zlatić et A. C. Hewson, Éd., *Properties and Applications of Thermoelectric Materials*. Dordrecht: Springer Netherlands, 2009.

[20] V. K. Zaitsev, M. I. Fedorov, I. S. Eremin, et E. A. Gurieva, « Thermoelectrics on the base of solid solutions of Mg2BIV compounds (BIV = Si, Ge, Sn) », in Thermoelectrics handbook: macro to nano, 2006eéd., D.M. Rowe, p. 29–1.

Bibliography

CHAPTER 2

[1] A. Al Alam, « Modélisation Au Sein De La Dft Des Propriétés Des Structures Electronique Et Magnétique Et De Liaison Chimique Des Hydrures D'intermétalliques ». 2009.

[2] N. Richard And C. E. A. Dam, "Actinides Et Terres Rares Sous Pression: Approche Pseudopotentiel," P. 12.

[3] A. Mickiewie, "A New Formulation," Vol. 111, No. 5, Pp. 217–219, 1985.

[4] J. C. Slater, "The Theory Of Complex Spectra," Phys. Rev., Vol. 34, No. 10, Pp. 1293–1322, 1929.

[5] R. O. Jones, "Density Functional Theory: Its Origins, Rise To Prominence, And Future," Rev. Mod. Phys., Vol. 87, No. 3, 2015.

[6] W. Kohn And L. J. Sham, "Self-Consistent Equations Including Exchange And Correlation Effects," Phys. Rev., Vol. Volum E 14, No. 1951, 1965.

[7] W. Kohn And L. J. Sham, "Self-Consistent Equations Including Exchange And Correlation Effects," Phys. Rev., Vol. Volum E 14, No. 1951, 1965.

[8] « D.M. Ceperley, B.J. Alder. Phys. Rev. Lett. 45, (1980) 566. »

[9] J. P. Perdew, K. Burke, And M. Ernzerhof, "Generalized Gradient Approximation Made Simple," Phys. Rev. Lett., Vol. 77, No. 18, Pp. 3865–3868, 1996.

[10] F. Tran And P. Blaha, « Accurate Band Gaps Of Semiconductors And Insulators With A Semilocal Exchange-Correlation Potential », P. 4, 05-Juin-2009.

[11] L. Badding, « Calcul Ab-Initio Des Propriétés Physiques De Quelques Nouveaux Matériaux Potentiels Pour L'optique Non Linéaire Quadratique », 2015.

[12] S. Richard, « Etude-De-Premier-Principe-Des-Propretes-Structurales-Optiques-Et-Thermodynamiques-Des-Composes.Znm2x4(M=Ga, In Et X=Se, Te) Avec Les Structures Dites "Defect Chalcopyrite" Et Defect Famatinite' », Abou Bekr Belkaid Tlemcen, 2017.

[13] T.J. Scheidemantel And C. Ambrosch-Draxl. « Transport Coefficients From First-Principles Calculations », P. 6, 2003.

Bibliography

CHAPTER 3

[1] Scheidemantel, T. J.; Ambrosch-Draxl, C.; Thonhauser, T.; Badding, J. V.; Sofo, J. O.Phys. Rev. B 2003, 68, 125210.

[2] J. P. Perdew, K. Burke, M. Ernzerhof. Phys. Rev. Lett. 77, (1996) 3865.

[3] T. Fabien and P. Blaha, « Accurate Band Gaps of Semiconductors and Insulators with a Semilocal Exchange-Correlation Potential », p. 4, 05-juin-2009.

[4] H .J. Monkhorst and J.D. Pack, Phys. Rev. B 13, 5188(1976).

[5] P. J, S. D J, A. S, M. D, D. A, et B. R, « Doping and temperature dependence of thermoelectric properties in Mg 2 (Si, Sn) », 2012.

[6] R. Hull, R. M. Osgood, Jr., H. Sakaki, et A. Zunger, « Thermoelectrics-Basic-Principles-and-New-Materials-Developments.pdf ». Springer Series in, 2001.

[7] C. Samira, « Etude des propriétés structurales, électroniques, thermiques et thermodynamiques des alliages ternaires BaxSr1-xS, BaxSr1-xSe et BaxSr1-xTe. », BADJI MOKHTAR, 2015.

General conclusion:

This work is aimed to study the contribution to the study of the structural, electronic, a transport property of solid solutions Mg2Si1-xSnx. For our study, we looked at the concentrations (x = 0, 0.25, 0.5, 0.75, 1) of these solid solutions at pressure (P = 5Gpa, 10Gap, 15Gpa). We used two calculation codes: BoltzTraP for the transport properties and the WIEN2K code for the other properties, by the augmented and linearized total potential plane wave method (FPLAPW).

At first, we put great importance on lattice parameter and atomic position (forces optimization for the solid solution is necessary due the change of atomic position) because with a well optimized structure we arrive to accurate physical properties. we focused on the study of structural properties by determining the mesh parameter and the bulk modulus and its derivative. The results obtained for our compounds are in good agreement with those determined theoretically and experimentally.

In a second step, the studies of the electronic properties were restricted to the analysis of the band structures. In addition to the PBE-GGA approximation, the mBJ approach has been used to obtain better precision in the calculation of the gaps in order to obtain values that can match those of the experiment.The calculations showed that the compounds Mg2Si1-xSnx (x = 0 and 1) have an indirect gap ($\Gamma \rightarrow X$) and the compounds Mg2Si1-xSnx (x = 0.25, 0.5, 0.75), have direct gap ($\Gamma \rightarrow \Gamma$), In addition, the use of the mBJ method brought a marked improvement of the gap compared to the GGA(PBE).

We also studied the total and partial state densities (DOS) of Mg2Si1-xSnx, and we were able to distinguish the type of atom and orbital formed between the different elements of each compound.

The latest modeling of this work performed with the semi-classical approach implement in the BoltzTraP code. It allows us to determine the thermoelectric parameters of the compounds Mg2Si1-xSnx (x = 0.0.25, 0.5, 0.75, 1) at pressure (P = 5Gpa, 10Gap, 15Gpa). We obtained the electrical and thermal electronic conductivity and the Seebeck coefficients which confirmed the high temperature range of these compounds.

This work supports the idea of solid solutions and pressure effects for improved potential materials for thermoelectricity, suggesting other solid solution such as Mg2X (X = Si, Sn, Ge) to improve their thermoelectric quality.

Abstract

Study of pressure effects on thermoelectric materials

In this work, we carried out a theoretical study using the augmented and linearized augmented plan wave method (FP-LAPW), based on the density functional theory (DFT) implemented in the WIEN2K code, to determine the structural and electronic properties of the compounds Mg2Si1-xSnx (x = 0.0.25, 0.5, 0.75, 1) at pressure (P = 5Gpa, 10Gap, 15Gpa), thus, the calculation of transport properties by semi-classical BoltzTraP methods. Exchange potential and correlation (XC) is processed by the generalized gradient approximation (GGA) and the modified Beck Jonhson approximation (mBJ).

Key words: Density Functional Theory (DFT) – thermoelectricity - Mg2Si - Mg2Sn

Résumé

Étude les effets de pression sur les matériaux thermoélectrique

Dans ce travail nous avons effectué une étude théorique en utilisant la méthode des ondes planes augmentées et linéarilisées (FP-LAPW), basé sur la théorie de la fonctionnelle de la densité (DFT) implémenté dans le code de WIEN2K, pour déterminer les propriétés structurales et électroniques des composés Mg2Si1-xSnx (x=0,0.25, 0.5, 0.75, 1) à pression (P=5Gpa, 10Gap, 15Gpa), ainsi, le calcul des propriétés de transport par des méthodes semi-classique BoltzTraP. Le potentiel d'échange et corrélation (XC) est traité par l'approximation du gradient généralisé (GGA) et l'approximation modifiée de Beck Jonhson (mBJ).

Mots clés : théorie de la densité de la fonctionnelle - thermoélectricité - Mg2Si - Mg2Sn

ملخص

دراسة تأثيرات الضغط على المواد الحرارية الكهربائية

في هذا العمل قمنا بإجراء دراسة نظرية باستخدام طريقة الموجة المستوية المعززة والموحدة (FP-LAPW) ، على أساس نظرية الكثافة الوظيفية (DFT) المدرجة في كود WIEN2K ، لتحديد الخصائص التركيبية والمركبات الإلكترونية $Mg_2Si_{1-x}Sn_x$ (x=1 ، 0.75 ، 0.5 ، 0.25.0) عند الضغط (5Gpa، 10Gap ، P = 15Gpa) ، وأيضا ، حساب خصائص النقل بطرق BoltzTraP شبه الكلاسيكية. تتم معالجة التبادل وإمكانات الارتباط (XC) عن طريق تقريب التدرج العام GGA(PBE) وتقريب (mBJ).

الكلمات المفتاحية : نظرية الدالة الكثافية – الكهروحرارية – Mg2Si - Mg2Sn